Journal of Volcanology and Geothermal Research 284 (2014) 106–121

Contents lists available at ScienceDirect

Journal of Volcanology and Geothermal Research

journal homepage: www.elsevier.com/locate/jvolgeores

Multiple timescales of cyclical behaviour observed at two dome-forming eruptions

Oliver D. Lamb [a,*], Nick R. Varley [b], Tamsin A. Mather [a], David M. Pyle [a], Patrick J. Smith [c,d], Emma J. Liu [e]

[a] Department of Earth Sciences, University of Oxford, South Parks Road, Oxford, OX1 3AN, UK
[b] Facultad de Ciencias, Universidad de Colima, Av. Bernal Díaz del Castillo #340, Col. Villas San Sebastían, C.P. 28045, Colima, Colima, Mexico
[c] Montserrat Volcano Observatory, Flemmings, Montserrat, West Indies
[d] Seismic Research Centre, University of the West Indies, St. Augustine, Trinidad & Tobago, W.I.
[e] School of Earth Sciences, University of Bristol, Wills Memorial Building, Queen's Road, Bristol BS8 1RJ, UK

ARTICLE INFO

Article history:
Received 22 March 2014
Accepted 21 July 2014
Available online 1 August 2014

Keywords:
Lava dome
Volcano-seismicity
Time-series analysis
Periodic behaviour
Volcán de Colima
Soufrière Hills volcano

ABSTRACT

Cyclic behaviour over a range of timescales is a well-documented feature of many dome-forming volcanoes, but has not previously been identified in high resolution seismic data from Volcán de Colima (Mexico). Using daily seismic count datasets from Volcán de Colima and Soufrière Hills volcano (Montserrat), this study explores parallels in the long-term behaviour of seismicity at two long-lived systems. Datasets are examined using multiple techniques, including Fast-Fourier Transform, Detrended Fluctuation Analysis and Probabilistic Distribution Analysis, and the comparison of results from two systems reveals interesting parallels in sub-surface processes operating at both systems. Patterns of seismicity at both systems reveal complex but broadly similar long-term temporal patterns with cycles on the order of ~50- to ~200-days. These patterns are consistent with previously published spectral analyses of SO_2 flux time-series at Soufrière Hills volcano, and are attributed to variations in the movement of magma in each system. Detrended Fluctuation Analysis determined that both volcanic systems showed a systematic relationship between the number of seismic events and the relative 'roughness' of the time-series, and explosions at Volcán de Colima showed a 1.5–2 year cycle; neither observation has a clear explanatory mechanism. At Volcán de Colima, analysis of repose intervals between seismic events shows long-term behaviour that responds to changes in activity at the system. Similar patterns for both volcanic systems suggest a common process or processes driving the observed signal but it is not clear from these results alone what those processes may be. Further attempts to model conduit processes at each volcano must account for the similarities and differences in activity within each system. The identification of some commonalities in the patterns of behaviour during long-lived dome-forming eruptions at andesitic volcanoes provides a motivation for investigating further use of time-series analysis as a monitoring tool.

1. Introduction

Many volcanoes form lava domes, which are characterised by the slow extrusion of highly viscous magma that accumulates on or near the vent and can form voluminous edifices. Dome growth eruptions are generally relatively long-lived, lasting from months (e.g. Kelut, Indonesia; De Bélizal et al., 2012) to centuries (e.g. Mount Merapi, Indonesia; Siswowidjoyo et al., 1995), and often involve multiple collapse and explosive episodes. The transition from effusive to explosive activity of a dome may be rapid, presenting significant challenges for forecasting and hazard mitigation (e.g. the 1990–1995 eruption of Mount Unzen, Japan, Nakada et al., 1999; and the 2010 eruption of Mount Merapi, Indonesia, Surono et al., 2012). To address this, investigations using multi-parameter datasets and improved analytical tools may provide insights into the processes governing these rapid changes in volcano behaviour, and thereby help reduce the hazard posed by lava dome eruptions.

Periodic behaviour is commonly observed in eruption-related seismicity, ground deformation and in rates of degassing from volcanic systems; it has been documented in several volcanic systems including Santiaguito (Guatemala; Harris et al., 2003), Mt St Helens (USA; Swanson and Holcomb, 1990), and Soufrière Hills volcano (Montserrat; Voight et al., 1998; Loughlin et al., 2010; Wadge et al., 2010; Nicholson

Abbreviations: DFA, Detrended Fluctuation Analysis; FFT, Fast Fourier Transform; LALP, Low-amplitude, Long-period seismicity; MTM, Multitaper method; PDA, Probabilistic Distribution Analysis; PSD, Power Spectral Density; SHV, Soufrière Hills volcano; STFT, Short-term Fourier Transform; VdC, Volcán de Colima.

* Corresponding author at: Department of Earth, Ocean and Ecological Sciences, Jane Herdman Building, 4 Brownlow Street, Liverpool L69 3GP, UK. Tel.: +44 151 794 5160.
E-mail addresses: o.lamb@liverpool.ac.uk (O.D. Lamb), nick@ucol.mx (N.R. Varley), tamsin.mather@earth.ox.ac.uk (T.A. Mather), david.pyle@earth.ox.ac.uk (D.M. Pyle), paddy@mvo.ms (P.J. Smith), en12525@bristol.ac.uk (E.J. Liu).

http://dx.doi.org/10.1016/j.jvolgeores.2014.07.013

et al., 2013). Periodic behaviour can be relatively unstable, showing systematic or non-systematic temporal changes in nature as the eruption progresses (Denlinger and Hoblitt, 1999). Technological advances have permitted geophysical datasets to be studied at increasingly fine resolution, while advances in analytical methods and modelling have increased the sophistication of data interpretation (e.g. Odbert et al., 2014). Nevertheless, much of the previous work in this field has focused on individual volcanic systems and little work has been done to compare and contrast the geophysical and geochemical datasets from multiple well-monitored volcanoes (e.g. Varley et al., 2006; Watt et al., 2007; Lachowycz et al., 2013). One consequence of this is that there has been little translation of statistical techniques developed and applied at one volcano to other systems and, despite considerable endeavour, the potential use of time-series analysis and other statistical approaches to volcano monitoring has not yet been fully realised (e.g. Jaquet and Carniel, 2003; Jaquet et al., 2006).

At Soufrière Hills volcano, periodic variations have been observed in multiple geophysical datasets and used to construct models of the volcanic system (e.g. Voight et al., 1999; Costa et al., 2007b; Nicholson et al., 2013). In contrast, relatively little attention has been paid to comparable behaviour in datasets from Volcán de Colima (e.g. Lachowycz et al., 2013). Our study develops from that presented by Lachowycz et al. (2013), who applied Detrended Fluctuation Analysis to datasets from Volcán de Colima (2004–2009) and Soufrière Hills volcano (1997–2010). Here, we apply multiple statistical tools to volcano-seismic data from Volcán de Colima with the aim of identifying and describing systematic time-series variations prior to and during the 2007–2011 lava-dome formation. We also report a similar analysis on a volcano-seismic dataset from Phases 1, 2 and 3 (1996–2007) at Soufrière Hills volcano, Montserrat, allowing a direct comparison between the two systems. By using three analytical tools (Fast Fourier Transform, Detrended Fluctuation Analysis and Probabilistic Distribution Analysis) on two different volcanoes, this study will help attain a greater understanding of processes occurring during dome-forming eruptions and aims to identify what lessons learnt from the better studied Soufrière Hills volcano might be transferred to Volcán de Colima.

1.1. Field areas and Data

Volcanic activity is usually preceded and accompanied by seismicity, as the rock beneath the volcano responds to intrusion and flow of magma, and changes in stress (e.g. Sparks, 2003; Kilburn, 2012; Pyle et al., 2013). Volcano-seismicity is one of the most useful and widely monitored attributes of volcanoes and is well-established as a tool for understanding volcanic processes (Neuberg, 2000; McNutt, 2005; Chouet and Matoza, 2013). Seismic monitoring has yielded the most complete and well-populated time-series available for the volcanoes studied and is therefore the most appropriate dataset for the purpose of examining temporal behaviour. We have restricted our work to the analysis of data at a daily resolution for ease of processing, but acknowledge that there is significant potential for the analysis of higher temporal resolution data.

1.1.1. Volcán de Colima (VdC)

VdC is an andesitic stratovolcano located at the western end of the Trans-Mexico Volcanic Belt, lying approximately 30 km NNE of the city of Colima. Historical activity can be divided into ~100 year cycles dominated by dome growth and lava flows, with pyroclastic flows appearing shortly before the cycle ends with a major explosive eruption (e.g. 1818 and 1913; Luhr and Carmichael, 1980). The most recent eruptive activity has been ongoing since 1998, comprising at least five lava dome growth phases culminating in large Vulcanian explosions. Lava extrusion rates varied from a peak of 6–8 $m^3 s^{-1}$ in 2004 (Varley et al., 2010b) to 0.019 $m^3 s^{-1}$ in 2010 (Mueller et al., 2013). Smaller Vulcanian explosions and transient degassing events of variable magnitude and ash content also occurred at a rate of ~2–10 per day from March 2003 to July 2011 (Varley et al., 2010a,b; Lavallée et al., 2012). In July 2011 the volcano entered a quiescent period which ended in January 2013 with several large explosions heralding a new phase of activity. Small daily explosions resumed thereafter and a new dome and lava flow is ongoing as of June 2014.

During the recent eruptive activity there have been three dominant groups of seismicity at VdC: long-period and those due to explosions and rockfall. Explosion events are divided into impulsive and emergent events, and long-period seismicity is separated into (relatively) large long-period events, and short-duration, low-amplitude long-period (LALP) events (for more details see Table A, Supplementary File 1). We analyse both explosion and LALP events from January 2006 to July 2011 which includes the whole 2007–2011 dome-growth phase (2038 days; Fig. 1A). Seismicity associated with explosions is thought to be due to pressure release or pathway opening required for explosive venting of ash and/or gas. The source of long-period events has previously been modelled as deriving from a pressure differential and fluid movement (Chouet, 1996; Neuberg, 2000) but more recent work has described the source as brittle failure of magma as it passes through the glass transition, with resonance producing the low-frequency coda (Neuberg et al., 2006; Harrington and Brodsky, 2007; Varley et al., 2010a). The larger long-period events and rockfalls occur infrequently and have a relatively high degree of uncertainty during classification, thus precluding reliable time-series analysis. Events were manually classified and counted by the Centre de Intercambio e Investigación en Vulcanología (CIIV), Colima, by inspection of seismographs and spectrograms recorded by a short-period vertical seismometer (EZV4) located 1.7 km from the volcano's summit; the seismometer forms part of the Colima Seismic Network (RESCO; Arámbula-Mendoza et al., 2011). Constraints that arise from the network and its configuration are discussed in Section 1.1.3.

Hutchison et al. (2013) subdivided the 2007–2011 dome growth episode into three stages: the preliminary growth of a blocky lava dome (stage I, February 2007 to December 2007), endogenous dome growth with the formation of a large talus apron (stage II, January 2008 to February 2010), and the formation of a lava lobe and a change to exogenous growth (stage III, February 2010 to July 2011). These divisions are used here to relate changes in activity to any features that arise from analysis of the seismic time-series.

1.1.2. Soufrière Hills volcano (SHV)

SHV is an andesitic stratovolcano in the southern part of Montserrat, in the Lesser Antilles island arc. Activity since 1995 has been characterised by five phases of lava dome growth, the first three of which lasted 2–3 years separated by pauses of ~2 years. Active growth is typically dominated by lava extrusion interrupted by periodic explosive activity and dome collapses (Herd et al., 2005). Similar to VdC, there was explosive activity between each phase of active dome growth (Druitt et al., 2002; Norton et al., 2002), with occasional larger vulcanian explosions sometimes associated with dome collapse (Linde et al., 2010). Typical extrusion rates are higher at SHV, with a range of 0.2–5.6 $m^3 s^{-1}$ (Ryan et al., 2010; Wadge et al., 2010).

Explosive behaviour at SHV has often shown correlation with cyclicity in other parameters, improving the potential for forecasting during periods of activity, and leading to a better understanding of ongoing processes in the conduit (Pyle, 1998; Connor et al., 2003; Watt et al., 2007). A series of Vulcanian explosions in 1997 coincided with tilt cycle maxima and sub-daily seismic cycles (Voight et al., 1998). Studies of ground deformation and volcano-seismicity at SHV have described both sub-daily (3–30 h) and 6–8 week ('50-day') cycles (Voight et al., 1998; Odbert and Wadge, 2009; Loughlin et al., 2010). Cyclic behaviour is widely considered to be the result of competing processes in the system, with sub-daily behaviour explained by periodic stick–slip magma plug motion, in response to shallow-conduit pressurisation (e.g. Denlinger and Hoblitt, 1999; Melnik and Sparks, 2005; Costa et al., 2013). For the longer '50-day cycle', periodic expansion and

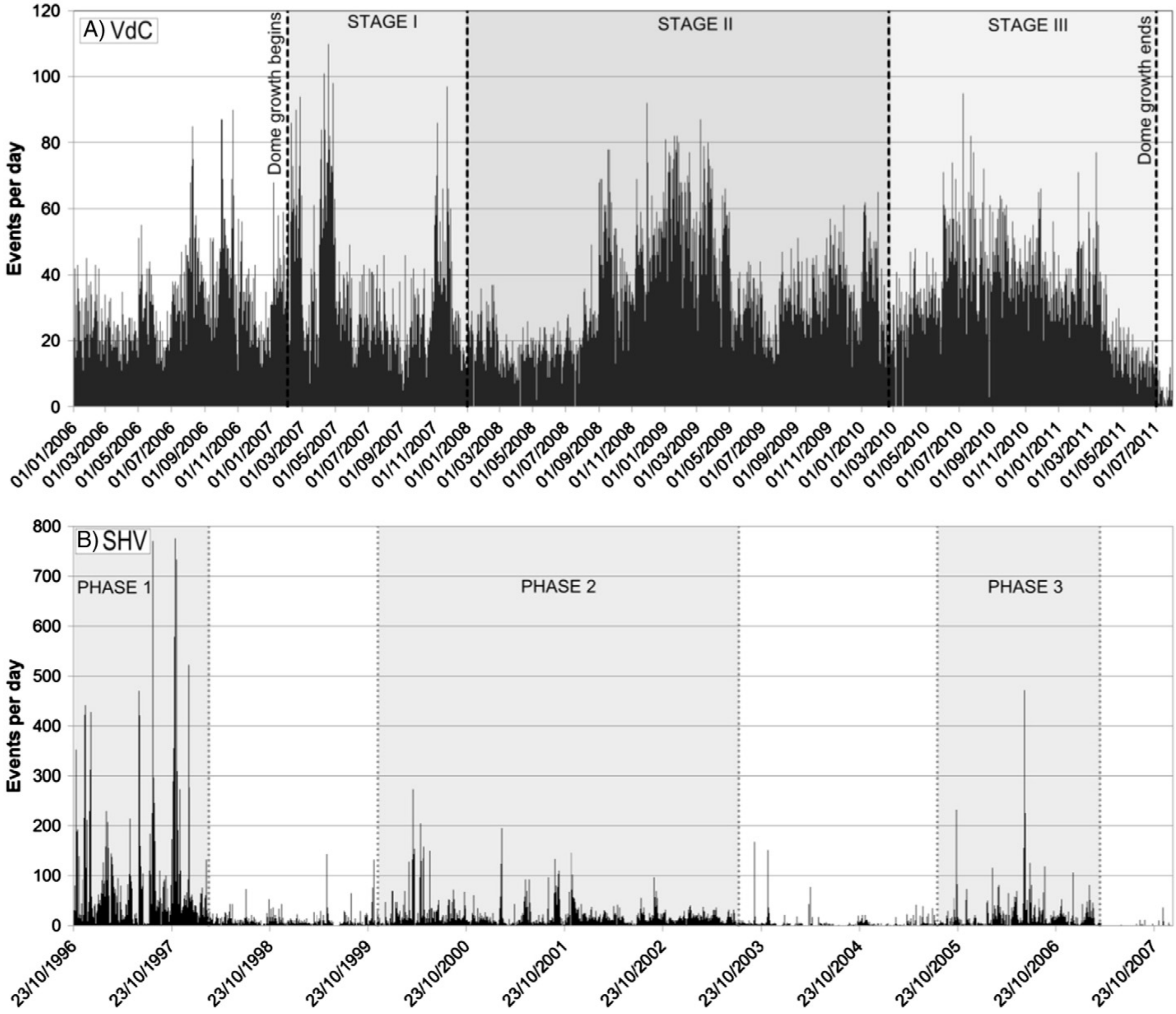

Fig. 1. Total daily counts for seismicity types analysed in this study from (A) Volcán de Colima (VdC) and (B) Soufrière Hills volcano (SHV); note the different y-axis scales. Classification of stages for VdC dataset is based on Hutchison et al. (2013). Phases of active dome growth at SHV are derived from Wadge et al. (2010); note that Phase 1 began on November 15 1995, before the start of the dataset.

contraction of an elastic-walled dyke, which acts as a volumetric capacitor to magma storage in the lower conduit, has been invoked (Costa et al., 2007a,b, 2013).

We analyse the daily counts of three observed volcano-seismic event types (hybrid, long-period, and volcano-tectonic; see Table B, Supplementary file 1) from October 1996 to December 2007 (4087 days; Fig. 1B). This period of analysis includes the three longest phases of activity at SHV (Phases 1, 2 and 3). Phases 4 and 5 are not considered here as their durations are too short for the associated seismic activity to be analysed robustly. Long-period and hybrid seismicity are thought to be related to resonance in the conduit triggered by brittle failure of ascending magma (Neuberg et al., 2006; Harrington and Brodsky, 2007). Volcano-tectonic seismicity is interpreted as fractures in the country rock caused by the intrusion of magmas (Chouet et al., 1994; Lahr et al., 1994). Rockfalls at SHV are not analysed here as it is not possible to compare with the poor rockfall record at VdC. Seismicity on Montserrat is recorded by a network of seismometers, both broadband and short-period, which transmit signals to the Montserrat Volcano Observatory by spread-spectrum radio (Luckett et al., 2007). Classification, counting and analysis of the seismic events are carried out daily by analysts at the observatory using SEISAN software, which has the facility to record signal subtypes (Luckett et al., 2007). Constraints that arise from the network and its configuration are discussed in Section 1.1.3.

1.1.3. Network constraints

Each volcanic system is host to a seismometer network which is used to constantly monitor activity as well as collect data for analysis. However, both networks are imperfect with sources of bias and error that merit discussion before analysing the datasets. Sources of bias that are common to both networks include:

- Background noise — Changes or increases in background noise due to weather/sea conditions can obscure smaller events, particularly during severe weather.
- Teleseismic events — Large local tectonic events are already accounted for in each network, but can still obscure a negligible number of small volcanic seismic signals.
- Operator bias — Misclassification of events, or changing of criteria

over time is something that is always present in manual classification of signals. At SHV, the most common errors are that between some hybrids and volcano-tectonic events, and hybrids and long-period events. At VdC, the most common errors are between emergent and impulsive events, and between true and false (i.e. short-lived noise) low-amplitude, long-period events.
- High activity — During periods of high activity the seismic signals are dominated by large numbers of rockfalls and/or pyroclastic flows which can obscure the smaller signals of greater interest. Similarly, the smaller signals can get swamped during a swarm of hybrid or long-period seismicity.

There is also a bias that derives from the configuration of the network, but they differ at each network:

- SHV — The network configuration on Montserrat (Luckett et al., 2008) has not remained the same throughout the period of analysis and the number of stations can affect the threshold used for automatic detection of events. The number of stations tends to go down during periods of high activity as stations are destroyed, or run out of power due to ash on solar panels, and cannot be repaired due to safety reasons. This kind of bias is inherent and is difficult to avoid as well as quantify. However, the similarity in timescale of the results here and with results from time-series analysis of other geophysical data streams (e.g. SO_2 flux; Nicholson et al., 2013) suggests this bias has a negligible effect on the analysis of the dataset.
- VdC — Events at VdC have been manually classified from a single short-period seismometer (EZV4) located 1.7 km from the active vent. If data from this station was unavailable then data from another short-period seismometer (EZV5), located 4 km from the vent, was used instead. The greater distance from the vent meant that smaller events, such as low-amplitude long period events, are more likely to be missed due to attenuation or obscuration by background noise. However, EZV4 was never unavailable for more than a week which means a minimal number of events could have been missed.

In conclusion, the datasets used here are not totally consistent records of the seismicity and results from their analysis must be interpreted with a degree of caution. The biases that are present are inherent and are nearly all unavoidable. Errors in manual classification can be minimized through training and strict criteria but the development of accurate automatic classification could mean that manual classification may not be relied upon in the future.

2. Methods

Time-series analysis offers a robust method of characterising long-term behaviour within geophysical systems. This approach also offers the potential for use in the long-term monitoring of restless or active volcanoes, for example in the automated identification of 'thresholds', or changes in the patterns of behaviour. Here three analytical techniques are used: Fast-Fourier Transform analysis, Detrended Fluctuation Analysis, and Probabilistic Distribution Analysis. Each method has been successfully applied to volcanic datasets in previous work (e.g. Watt et al., 2007; Odbert and Wadge, 2009; Lachowycz et al., 2013; Nicholson et al., 2013) but this study is the first to use all three approaches together to compare parallel volcanic systems.

2.1. Fast Fourier Transform (FFT)

Volcanic time-series are inherently non-linear and can show cyclicity over a range of timescales. Superposition of multiple cycles within a dataset can obscure the true signals. The Fast-Fourier Transform (FFT) offers an efficient means of examining the characteristics of a time-series (Danielson and Lanczos, 1942) via the Power Spectral Density (PSD) estimate (Percival and Walden, 1993), which highlights the power of periodic components in the signal. The PSD here is estimated using the Multitaper Method (MTM), demonstrated to be the most robust method when there is no prior knowledge of the signal-generating source (Thomson, 1982). The SSA-MTM Toolkit presented by Ghil et al. (2002) was used to perform the spectral analyses here. A detrending correction was used to prepare the data by rendering the time-series approximately stationary, then either padded with zeroes at either end or truncated to a length of n^2 samples, for integer n, as required for FFT. The significance of spectral peaks were assessed against a statistical red noise model (Mann and Lees, 1996), which is considered the most applicable characterization of background noise within geophysical systems where processes act over timescales greater than the selected sample length. It is impossible to fully characterise the nature of the noise without prior knowledge of the generating source; therefore the red noise model acts only as a guide to interpretation. Here peaks above the 95% confidence threshold are considered significant for discussion.

MTM analysis requires statistical stationarity over the whole data window, which is not a common feature of many geophysical systems and can result in spectra which are difficult to interpret. Short-term Fourier Transform analysis (STFT) calculates a series of PSD estimates using a moving window of specified length with results illustrated using spectrograms. An assumption of stationarity is only required within an individual sample window, therefore spectrograms are useful for tracking changes in the spectral content of a time-series (Odbert and Wadge, 2009). These results can be directly compared with other observations (e.g. magma effusion rate) during the time period of analysis which can help constrain the process giving rise to any cycles.

The choice of parameters (window length and window overlap) is critical and has been optimised for each analysis depending on the timescales of interest. A window length of 256 days with 99% overlap provided the best compromise between achieving sufficient temporal resolution and maintaining a long enough window for robust analysis. The frequency distribution of each window was normalised to unity in order to remove the influence of changes to absolute spectral power, thereby allowing direct comparison of the relative frequency distributions between contiguous windows. This represents a similar approach to that chosen by Nicholson et al. (2013) for datasets with a similar timescale and temporal resolution. For each analysis, a high-pass Butterworth filter (cut-off = 365 days; Butterworth, 1930) has been applied to the time-series prior to the spectrogram calculation to enhance the clarity of the shorter period cycles of interest. Comparison between spectrograms generated from both raw and pre-filtered data indicated that the use of a filter did not affect either the timing or the frequency of resulting spectral peaks. However, the filter cannot remove the effects of long-periods of time with little or no seismicity (e.g. March 1998 to November 1999 at SHV). Exclusive STFT analysis of October 1996 to March 1998 (thus excluding periods of low seismicity) at SHV produced a similar result to that observed when the whole-time-series (which includes periods of low seismicity) was analysed, indicating that periods of low seismicity do not distort results. These methods have not previously been used at VdC but have been used extensively on geophysical datasets from SHV. Odbert and Wadge (2009) applied both MTM and STFT analysis to tiltmeter deformation time-series and found two cycles (9 h and 3 days), one of which was previously unknown. Nicholson et al. (2013) identified and tracked temporal changes in periodicity of SO_2 degassing rates at SHV and demonstrated that the strength of cyclicity (multi-year and ~50-day timescales) varied systematically with respect to the style of eruptive activity.

2.2. Detrended fluctuation analysis (DFA)

DFA has the potential to identify structure in the time-series that has not been highlighted by FFT, enabling additional constraints to be placed on the nature of sub-surface processes. DFA is used to quantify the nature of long-range correlations in non-stationary signals (Peng et al., 1994). The resulting scaling exponent (α) quantifies the long-range correlation properties of the time-series and can take values ranging from 0 to ~1.5. Values in the range $0 < \alpha < 0.5$ signify alternating large and small values are more likely (i.e. anti-persistence). If $\alpha \cong 0.5$, each value is not correlated with any previous values (i.e. white noise). $0.5 < \alpha < 1$ indicates long-range power-law correlation (i.e. persistence), such that a value is more likely to be followed by similar values. $\alpha \cong 1$ indicates strongly persistent, period-like ('pink') noise and if $\alpha > 1$, strong correlations exist, but are not of a power-law form. A value of $\alpha \cong 1.5$ would result from 'red' (Brownian) noise, i.e. random walk-like fluctuations in the signal through time. In simple terms, α may be considered as a measure of the 'roughness' of a time-series: the higher the scaling exponent, the 'smoother' the time-series (Peng et al., 1994). A more detailed methodology, including an explanation of how α is calculated, is presented in Lachowycz et al. (2013). Here we investigate the temporal variation of α using a moving window approach, following the method of Alvarez-Ramirez et al. (2009) and Lachowycz et al. (2013). α is calculated for a subset of the data of a specified length that is run incrementally through the time-series.

The parameters that must be considered are the moving window size, the range of box sizes to calculate α and the moving increment. One notable feature between different box sizes is a short-term cycle superimposed onto long-term trends, with the cycle period scaling with the maximum box size, indicating that a parameter artefact distorts the results at short timescales. This artefact has been observed before and was explained by the influence of small variations in the dataset and the moving increment; when there is insufficient variability in the exponent time-series, a box/window-shift cycle effect is not masked by the influence of new data included in the window as it is moved (Lachowycz et al., 2013). Here, we find that long-term trends on scales greater than the maximum box size are independent and can be isolated by using a moving increment larger than the maximum box size. Considering the disorder of the correlation above a box size of 100 days ($\log(n) = 2$; see Section 3.2 and Fig. 2) and the artefact discussed above, the parameters chosen for this analysis are a 180-day moving window with a 45-day maximum box size and a 50-day increment.

DFA has previously been successfully applied to datasets from multiple volcanic systems. Analysis of the hourly time variation in volcano-magnetic signals recorded at Mt. Etna (Italy) revealed two distinct scaling regions as well as cyclic variation on multiple timescales (Currenti et al., 2005). Alvarez-Ramirez et al. (2009) used DFA to quantify correlations in an explosion time-series from Popocatépetl volcano (Mexico) with results showing two quasi-periodic cycles (0.22 and 1.2 year) which they linked to volcano-tectonic events. As mentioned before, Lachowycz et al. (2013) tested the technique on seismic data (real-time seismic amplitude/energy measurements and event counts) from VdC (2004–2008) and SHV (1996–2011).

2.3. Probabilistic distribution analysis (PDA)

As volcanic events can be treated as a stochastic time-series and modelled by fitting statistical distributions, probabilistic estimates of variables such as repose intervals can be made. Here we use the Weibull model, which is commonly used in failure analysis, and the log-logistic model, which is used to model systems involving multiple competing processes. The cumulative distribution functions, $F(x)$, for each model are given below:

$$\text{for}: \ 0 \le x < \infty; \ a > 0; \ b > 0$$

$$\text{Weibull}: F(x) = 1 - \exp\left[-(x/b)^a\right]$$

$$\text{Log-logistic}: F(x) = 1/\left[1 + (x/b)^a\right].$$

Parameters a and b are difficult to define physically; the shape parameter, a, can be related the overall distribution shape, whereas b, the scale parameter, can be thought of as an approximation to the mean (Weibull) or median (log-logistic) of the system.

Previous work using this method has generally concentrated on the analysis of time intervals between Vulcanian explosions. Connor et al. (2003) found that inter-explosion timescales at SHV fit well with the log-logistic distribution. However, Watt et al. (2007) found that while the log-logistic model fits some explosion datasets, the Weibull model provided a better fit to inter-explosion intervals from some other volcanic systems, and suggested that rates of magma ascent and pressurisation within the conduit may be the most important controls in determining the distributions of repose intervals in Vulcanian systems. Varley et al. (2006) modelled repose intervals probabilistically

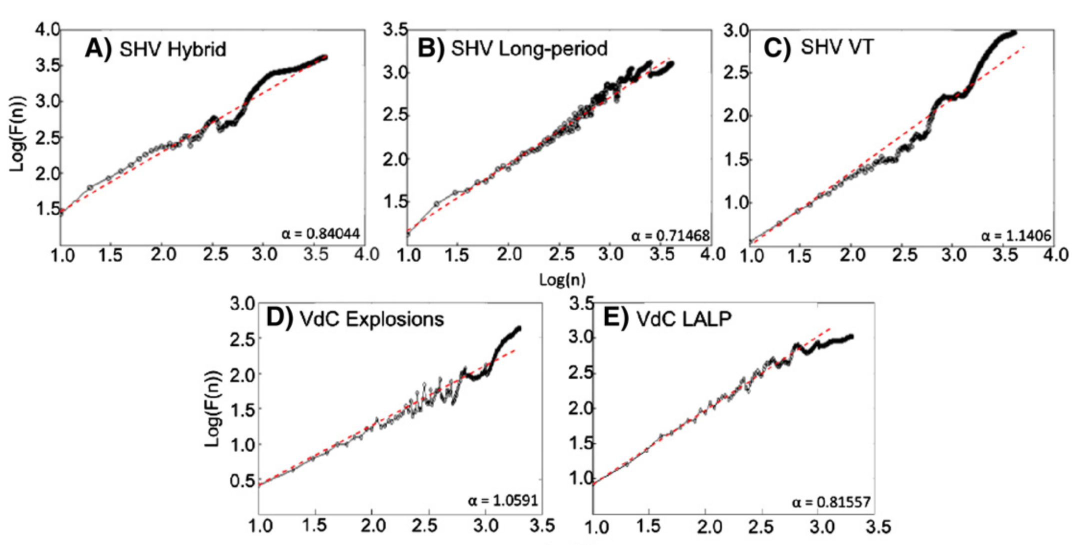

Fig. 2. Log-logarithmic plots of fluctuation function against box-size resulting from Detrended Fluctuation Analysis (DFA) of Soufrière Hills volcano (SHV) and Volcán de Colima (VdC) time series. From SHV, (A) Hybrid, (B) Long-period, and (C) Volcano-tectonic events. From VdC, (D) explosion time series, and (E) Low-amplitude Long-period (LALP) events. α is the gradient of the line calculated by least-squares regression, represented by the dashed red line.

using survival functions at four volcanic systems, including VdC. Their results showed that activity can be divided temporally into different phases which aided the construction of a model to explain variations of eruptive activity.

Here we apply PDA to the repose intervals between discrete seismic events at VdC, with each time-series divided into bins with an equal number of events in each. The statistical distribution parameters, *a* and *b*, were estimated for each bin by using both the maximum likelihood method and probability plots (Fig. 3A, B). Goodness of fit between the repose interval distribution and the statistical distributions was found by calculating the Kolmogorov–Smirnov *P*-values (range: 0–1; Massey, 1951) that give the probability that the observed data were generated by a particular model. Here we use the criterion that $P > 0.8$ to suggest that a model is a good description of the data. By tracing the variation in *P*-values for each model over the time-series, temporal variation in the processes affecting the seismicity can be described.

We applied this method only to the VdC dataset since the SHV dataset did not include the repose periods between discrete seismic events; it only included the day by day counts of each type of seismic event at the volcanic system. Although it is possible to use calculated average repose intervals per day this can produce unreliable probability curves (Watt et al., 2007). In the VdC dataset, the repose intervals for Impulsive and Emergent events were not combined as for the purpose of this particular method they are considered statistically independent (Varley et al., 2006).

3. Results

3.1. Fast Fourier Transform

3.1.1. Multi-taper method

MTM analysis was carried out on all complete seismic event count time-series to provide a first-pass assessment of the cyclic character of the dataset (Fig. 4; Tables 1a, 1b). Each PSD estimate reveals multiple peaks of variable width and amplitude that appear significant above the 95% noise confidence thresholds. Spectral peaks with periods of 23–28 and 41–47 days are common to all time-series. All time-series also show variable numbers of peaks corresponding to 50–100 day cycles. Cycles with periods >100-days are a feature of all datasets, with the exception of the explosion time-series from VdC. Most of these cycles are represented by the maxima of relatively broad peaks in the PSD, which often indicate temporal variation in cycle frequency; this implies that the cycles are either unstable or are a possible artefact of the analysis.

Analyses of subsections of the complete time-series (Tables 1a, 1b; Figures A, B, Supplementary file 2) are broadly consistent with the results obtained when the whole time-series is considered. However, although the dominant frequencies identified in the analysis of the complete time-series (Fig. 4) are also evident on Figures A and B, the exact frequencies and relative importance of cycles vary between successive subsections (i.e. cyclic components are not persistent throughout the time-series). The broad nature of the spectral peaks in the whole-

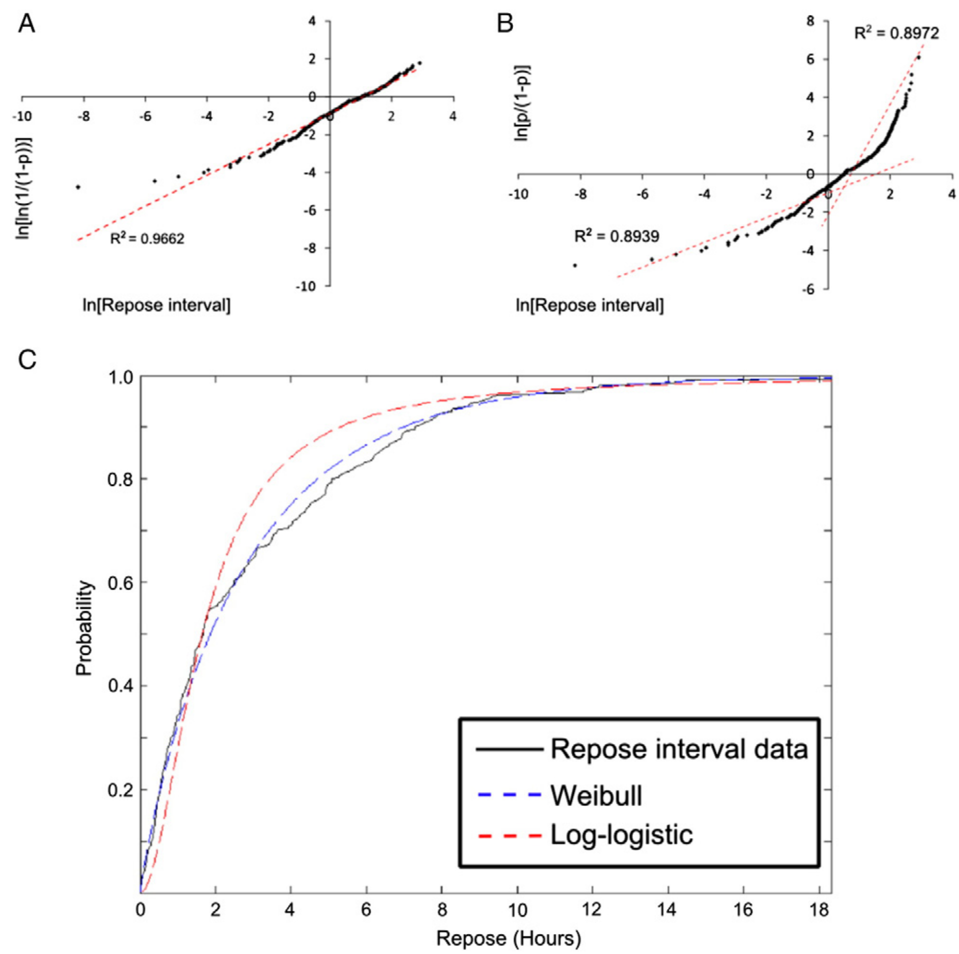

Fig. 3. Examples of probability graphs (A and B) used to estimate the parameters for the Weibull and log-logistic models. C is an example of a cumulative distribution plot showing the repose interval plot with the Weibull and log-logistic models plotted against it. All three graphs are calculated from repose intervals of Emergent events between 03/09/10 and 28/10/10 at Volcán de Colima.

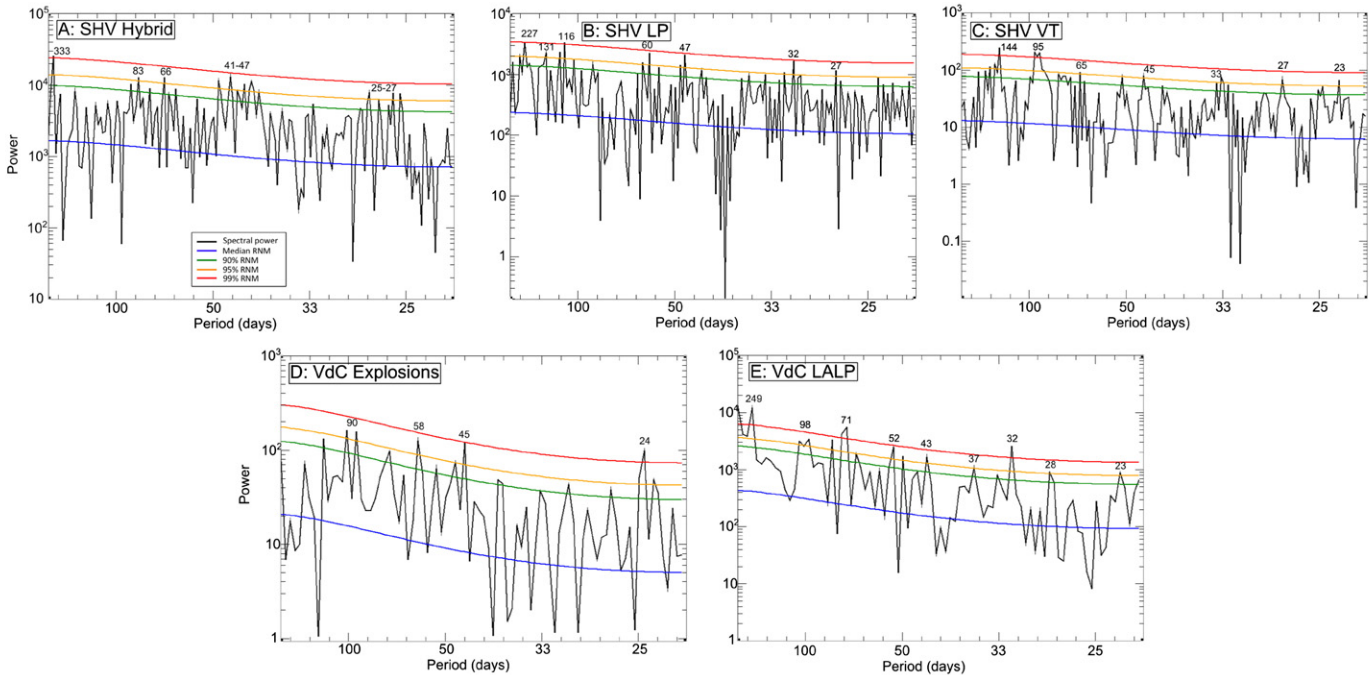

Fig. 4. MTM spectra showing whole time-series power spectral density (PSD) of the daily event counts (1996–2007 and 2006–2011 at SHV and VdC, respectively) for (A) hybrid, (B) long-period, (C) volcano-tectonic events from SHV, and (D) explosions and (E) LALP events during from VdC. PSD is plotted against various confidence levels of the Red Noise Model. Peaks exceeding at least the 95% confidence level are annotated with the corresponding cycle period in days.

time-series analysis is therefore a reflection of temporal instability in cyclicity at VdC and SHV. Given that the two volcanic systems are governed by complex interactions between multiple processes and feedbacks operating on various timescales, this is not an unexpected result.

These results show the cyclic behaviour at VdC occurs on a range of timescales, and in a number of different seismic monitoring datasets (Tables 1a, 1b). However, several observations, including broad spectral peaks (Fig. 4) and inconsistency in absolute cycle length and/or dominance between analyses of successive subsections (Figures A and B, Supplementary file 2), indicate that individual components are not always persistent throughout the time interval of analysis. Although this cyclic instability brings into question the assumption of statistical stationarity (required by definition for MTM spectral analysis) the alternative method of STFT analysis only requires the time-series to remain stationary within each 'window' (described in Section 2.1). We have therefore applied the STFT approach to explore the temporal variability of the time-series in more detail; results from each volcanic system are described below.

3.1.2. Short-term Fourier Transform

Preliminary inspection of the spectrograms from the VdC datasets (Fig. 5) highlights sub-annual cycles which fluctuate in strength through the time-series:

- Explosions — For explosion events (Fig. 5A), the daily counts are dominated by a ~100-day cycle almost throughout. During late 2008, there is a brief period where a 50-day cycle is evident but no correlation is apparent with the dome-growth patterns highlighted by Hutchison et al. (2013; see Section 1.2.1). A switch from endogenous to

Table 1a
Summary of MTM analysis results for Volcán de Colima (VdC). Cycles are described by their period (days) and classified based on the level of confidence at which this peak exceeds the Red Noise Model. Cycles in italics are those that are clearly seen in the spectrograms produced by the STFT analysis (Section 3.1.3).

VdC	2006–2011 (2038 samples)		Before effusion (399)		Stage I (332)		Stage II (781)		Stage III (495)	
Confidence Level (%)	99	95	99	95	99	95	99	95	99	95
Explosions	24	90, 58, 45		*31*		24	46	73, *25*	*102, 25*	
LALP	333, 250, 71, 32	100, 52, 43, 37, 28, 23	85, 48	21	68	32		68, *32, 24*		78, 25

Table 1b
Summary of MTM analysis results for Soufrière Hills volcano (SHV). Cycles are described by their period (days) and classified based on the level of confidence at which this peak exceeds the Red Noise Model. Cycles in italics are those that are clearly seen in the spectrograms produced by the STFT analysis (Section 3.1.3).

SHV	1996–2007 (4087 samples)		Phase 1 (505)		Phase 2 (1348)		Phase 3 (604)	
Confidence level (%)	99	95	99	95	99	95	99	95
Hybrid	333	83, 66, 47, 45, 43, 41, 27, 26, 25	*78*, 21	*42*, 25		512, *54, 33, 29*	36	54, 28, 20
LP	227, 116	131, 60, 57, 47, 32, 31, 27	*205*, 21	*45*, 35	227, 158, 48	85, *59, 44*, 31, 27, 24, 22		35, 31, 23
Volcano-tectonic	144, 95	65, 45, 33, 27, 23	26	*171*	*186, 30, 23*	*35, 25, 22, 21, 20*	22	*34*, 26

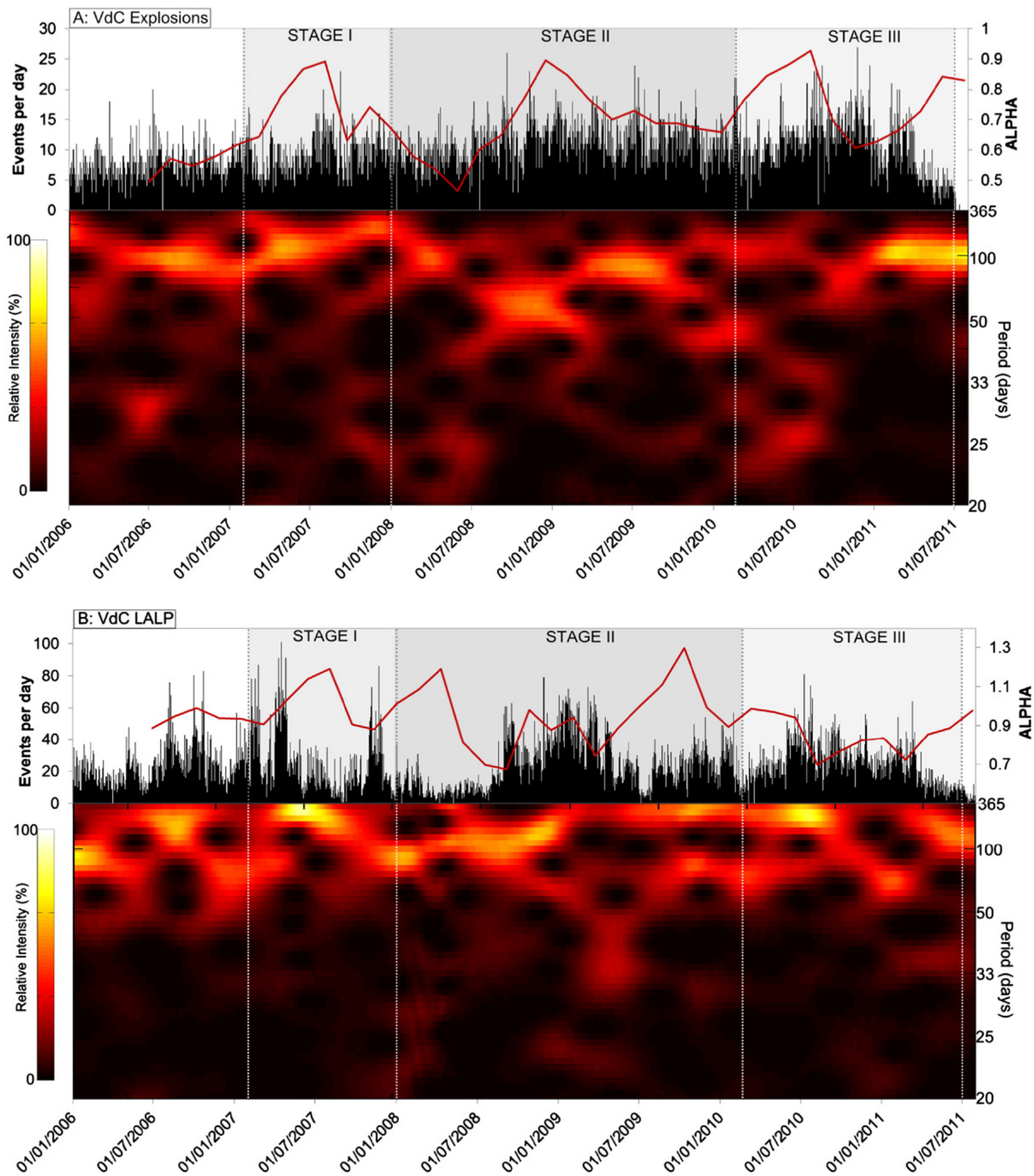

Fig. 5. Daily event counts (black bars), DFA scaling exponent (α) values (solid red line), and STFT spectrograms (lower half) for (A) explosion seismicity, and (B) LALP seismicity from Volcán de Colima (VdC). Note the differences in scales of y-axes. The scaling exponent (α) values are plotted at the end of their respective windows of measurement; gaps represent periods where invalid scaling exponents are calculated due to insufficient seismic events. Spectrograms are plotted from 20- to 365-day cycle periods; the maximum defined by the high-pass Butterworth filter. Regions of high intensity close to or on the maximum period represent intervals in the time-series where very low-frequency cycles or no cycles are measured. The power spectral density of each window has been normalised to unity.

exogenous growth in early 2010 (stage III) was followed by a period where no strong cyclic behaviour could be easily discerned. However, a brief and weak ~25-day cycle at the beginning of the stage correlates with the 25-day peak in the PSD of this subsection from MTM analysis (Table 1a; Figure A, Supplementary file 2).

- LALP events — For LALP events, the spectrogram (Fig. 5B) appears to be less ordered with cycles of 50- up to 200-days fluctuating in strength throughout the entire time-series. In mid-2009 there is a period where a weak 33-day cycle appears simultaneously with a decrease in the number of events per day; this correlates with the 32-day peak identified in the MTM analysis over stage II (Table 1a).

On first inspection, the spectrograms of the time-series from SHV appear to show more complex temporal variation than those from VdC:

- Hybrid events — The spectrogram for Hybrid events (Fig. 6A) shows no strong cycles of seismicity. On closer inspection, however, weak 50- and 100-day cycles can be discerned during Phase 1 of the activity. Just before the beginning of Phase 2, there is a hint of a brief weak 100-day cycle above the noise. Evidence of a 50-day cycle also appears in the middle of Phase 2, centred approximately on October 2001. Hybrid events continue after the end of Phase 2, and here we can see 50-day cycles briefly manifest although this is at the limit of

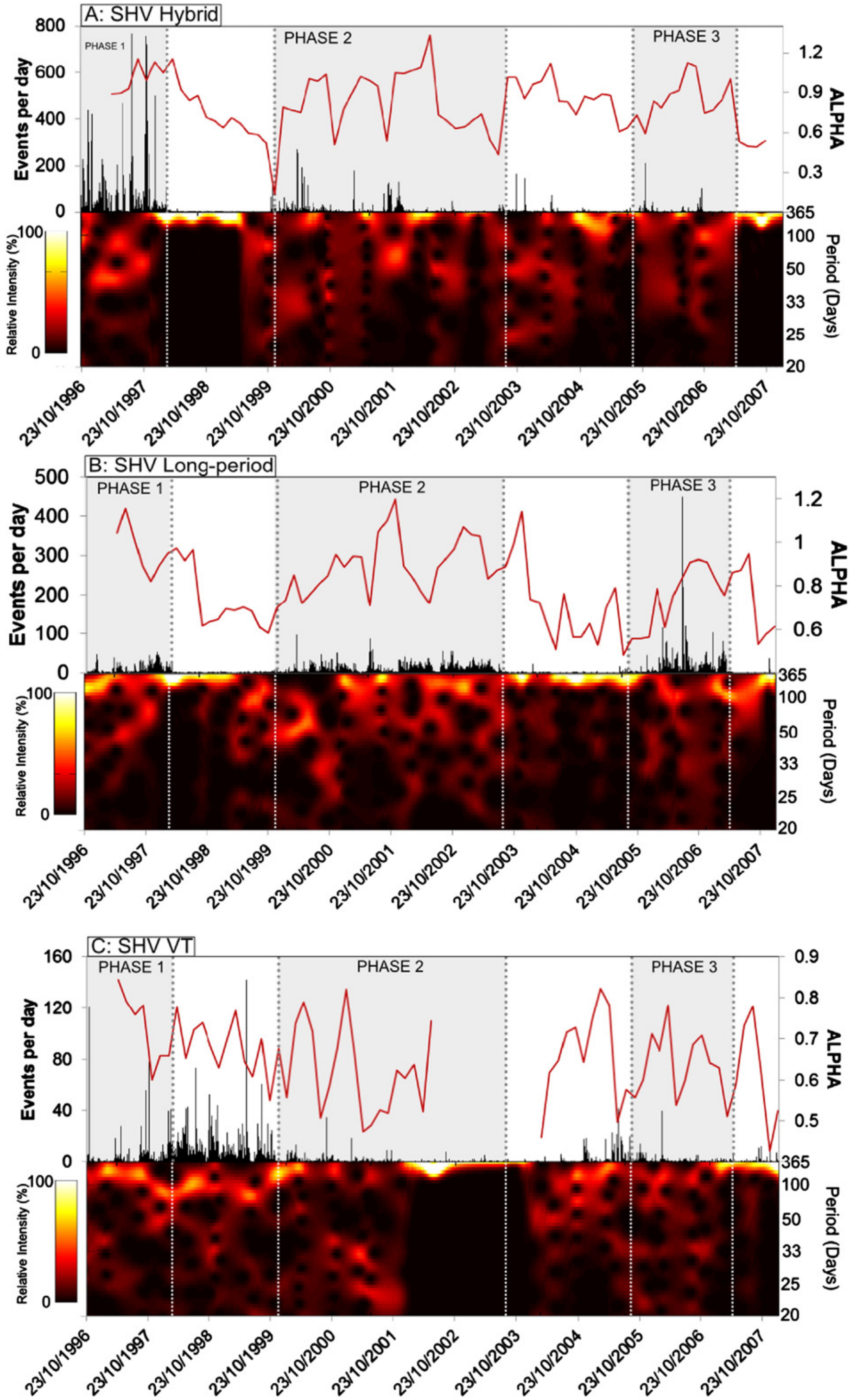

Fig. 6. Daily event counts (black bars), DFA scaling exponent (α) values (solid red line), and STFT spectrograms (lower half) for (A) hybrid, (B) long-period, and (C) volcano-tectonic (VT) event types from Soufrière Hills volcano (SHV). Note the differences in scales of y-axes for all three event types. The scaling exponent (α) values are plotted at the end of their respective windows of measurement; gaps represent periods where invalid scaling exponents are calculated due to insufficient seismic events. Spectrograms are plotted from 20- to 365-day cycle periods; the maximum defined by the high-pass Butterworth filter. Regions of high intensity close to or on the maximum period represent intervals in the time-series where very low-frequency cycles or no cycles are measured. The power spectral density of each window has been normalised to unity.

what can be distinguished from the noise. In the second half of Phase 3 the 100-day cycle is once again briefly evident at low intensity.

- Long-period events — In contrast to hybrid events, the spectrogram for long-period events (Fig. 6B) indicates that the seismicity is sporadically dominated by 100-day cycles during each phase of activity. A 50-day cycle can also be discerned in the middle of Phase 1 (May/June 1997) and the beginning of Phase 2 (January/February 2000). A brief 30-day cycle also appears during Phase 2 centred on October 2000.
- Volcano-tectonic events — For volcano-tectonic events (Fig. 6C), cycles are detected with 100- to ~200-day periods. The time variation of the

cyclicity from 1996 to 2002 suggests a relation between the level of activity at the volcano and the cycle frequency, with the 100-day cycle appearing during the pause between Phase 1 and 2 but the ~200-day cycle being stronger in Phase 1 itself. Seismicity from January 2004 to the end of Phase 3 in early 2007 shows a weak indication of a 200-day cycle.

3.1.3. FFT methodology comparison

By comparing and contrasting the results from MTM and STFT analysis, it is possible to evaluate the interpretations of each set of results as well as gain insights into the strengths and weaknesses of each method. We note that it is important to remember that MTM analysis produces one PSD from a time-series, while the spectrograms produced by STFT analysis represent the combination of many smaller PSDs from overlapping sections of the same time-series. Spectral peaks that are seen in the MTM results are sometimes not seen in the STFT spectrograms and vice versa.

For the time-series from VdC, the results do generally agree but there are a few cycles which are not seen by the other method.

- Explosion events — For the explosion events time-series from VdC, the ~100-day cycle seen in the spectrogram (Fig. 5A) is generally missing in the MTM results, with the exception of stage III (Table 1a). Smaller cycles in the subsections of the MTM analysis are seen in the spectrograms: the 31-day cycle from before effusion is seen mid-2006; the 25-day cycle in both stages II and III can be seen at the beginning of each stage, although it is stronger in the latter.
- LALP events — For LALP events, the ~100-day cycle in the spectrogram (Fig. 5B) is also missing in each subsection of the MTM analyses, but is seen in the PSD from whole time-series analysis (Table 1a). Cycles in the MTM analysis that can be seen in the spectrogram include the 32- and 24-day cycles in stage II (seen early to mid-2009), and the 78-day cycle in stage III (January 2011). However, there are also cycles in the MTM analysis that cannot be seen in the spectrogram: the 48- and 21-day cycles from before effusion, the 68- and 32-day cycle in stage I, and the 25-day cycle in stage III.

The results from both methods on the time-series from SHV show a greater degree of complexity than those at VdC.

- Hybrid events — Only five of the cycles seen in the MTM analysis of subsections of the Hybrid event time-series (Table 1b) can be clearly discerned in the STFT spectrogram (Fig. 6A). The 42- and 78-day cycles can be seen dominating Phase 1, but the 25-day cycle cannot be discerned from background noise and the 21-day cycle cannot be seen at all. In Phase 2, the 33- and 29-day cycles are seen weakly in late 1999 and the 54-day cycle can be seen in the strong patch centred on October 2001; the 512-day cycle is beyond the limits imposed by the high-pass Butterworth filter. None of the peaks highlighted by MTM analysis in Phase 3 are seen in the spectrogram, and a weak >100-day cycle in the spectrogram is not present in the MTM analysis results.
- Long-period events — For long-period events, both methods highlighted particularly complex temporal patterns such as those seen in Phase 2 (Fig. 6B; Table 1b). During this phase, only the 44- and 59-day cycles are clearly seen with a strong patch appearing in late 1999, and the 158- and 227-day cycles are hard to discern but could correlate with the patch seen during 2002. The other cycles identified by MTM analysis during this phase are hard to pick out from the background 'honeycomb' pattern. For Phase 1, only the 205- and 45-day cycles can be picked out, and in Phase 3 none of the MTM cycles can be clearly discerned.
- Volcano-tectonic events — In contrast to the other time-series, the results from the volcano-tectonic events suggest it is not as temporally complex (Fig. 6C; Table 1b). In Phase 1, the 171-day cycle is likely the strong patch dominating the spectrogram from late 1996 to mid-1997; the 26-day cycle is difficult to discern from the background levels. In Phase 2, the 186-day cycle is seen briefly in the strong patch at the very beginning of the phase in October 1999; the remaining cycles (20 to 35-day) are likely to be found in the weak patch from October 2000 to October 2001. The MTM cycles in Phase 3 are difficult to see against the background patterns in the spectrogram.

Comparing and contrasting the results from MTM and STFT analysis has brought up several key observations. Firstly some cycles seen in the results from one method are not seen in the results from the other. Secondly, cycles that do appear in both sets of results only appear transiently. Thirdly, if multiple cycles from MTM analysis of a subsection appear in the equivalent section in the spectrogram, the cycles are often not simultaneous (e.g. the 25- and 100-day cycle in stage III of the Explosion time-series from VdC; Fig. 5A and Table 1a). These observations and their implications are discussed below in Section 4.1.

3.2. Detrended fluctuation analysis

Like STFT, parameter selection for this method must be optimised to ensure reliable results. The moving window size must ensure maximum resolution while producing valid scaling exponents. Any trends in the scaling exponents must be independent of window size and moving increment and the box sizes must give log-log plots appropriate for calculating α. Each time-series was initially analysed with DFA to produce log-log plots to assess the correct parameters needed (Fig. 2).

Log-log plots were calculated with n ranging from 10 to m days, where m is the size of the dataset rounded down to a multiple of 10 (2040 for VdC, 4080 for SHV). The plots indicate that each time series is self-similar, displaying persistent behaviour on timescales of <100 days (Fig. 2); irregularity in log (F (n)) above log (n) $\approx$ 2 in all plots suggest disorder at >100 days. This constrains the maximum box size to 100 days, as values above this would give unreliable scaling exponents. The log-log plot for LALPs shows a break in slope at ~log (n) = 2.7, suggesting a change in scaling dynamics at >500 days. This was not observed in the log-log plots for the same seismic event type in Lachowycz et al. (2013); this is likely due to the longer time-series used here (we analyse January 2006 to July 2011, whereas Lachowycz et al. (2013) analyse November 2004 to December 2008).

3.2.1. Volcán de Colima

The scaling exponent for Explosion events remains within $0.5 < \alpha < 1$ indicating that the time-series is relatively persistent (Fig. 5A). For LALP events, α fluctuates between 0.7 and 1.3, moving from long-range power-law correlation to strong non-power-law correlations via 'pink noise' (Section 2.2; Fig. 5B). For both time-series there is no significant difference in α before and during dome growth. In the Explosion time-series a weak 1.5–2 year cycle can be seen which cannot be correlated with variations in volcanic activity. In the LALP time-series there is a 200- to 350-day cycle which requires further analysis.

3.2.2. Soufrière Hills volcano

The temporal variation of the scaling exponent for all three time-series at SHV ranges from strongly persistent values ($0.5 < \alpha < 1$) up to strong correlations not of a power-law form ($\alpha > 1$; Fig. 6). The scaling exponent for Hybrid seismicity appears to show little correlation in relation to changes in activity, with the exception of the significant dip immediately prior to Phase 2, but a weak annual cycle is observed during Phase 2 (Fig. 6A). For LP events, the temporal variation of α does appear to show a relation to activity, with higher values ($\alpha > 1$) during phases of activity, and a weak annual cycle during Phase 2 (Fig. 6B). Like the seismicity itself, the temporal variation of the scaling exponent for volcano-tectonic events shows no correlation with activity at the volcanic system (Fig. 6C). Instead, α values show a general and gentle downward trend with annual cycles appearing in the latter half of the time-series (January 2004 to December 2007).

3.3. Probabilistic distribution analysis

At Volcán de Colima both Impulsive and Emergent events show a peak in the *P*-value (the measure of goodness-of-fit) for the Weibull curve during Stage I and the start of Stage III (Fig. 7A, B). Outside of these time-periods, neither probabilistic model produces significant *P*-values. For LALP events there are correlations between activity at VdC and the pattern of the *P*-values (Fig. 7C). In early 2006 we see a strong fit to Weibull models, superseded by a stronger log-logistic curve in the first half of 2007. As the dome growth continues from 2007 to mid-2011, the *P*-value for the Weibull curve increases gradually up to high values of >0.9. This suggests a transition from one dominant process to another and the log-logistic period represents the overlap between these processes; this is discussed further in Section 4.3.

4. Discussion

4.1. Common seismic cyclicity

MTM analysis of the complete time-series revealed complex seismicity patterns at both SHV and VdC, providing evidence for multiple superimposed cycles during phases of activity (Fig. 4). The broad nature of many of the spectral peaks suggested temporal variability of the cycles which was subsequently confirmed from MTM analysis of subsections of each time-series (Tables 1a, 1b; Figure A, B in Supplementary file 2). This is similar to the results shown by Nicholson et al. (2013) from MTM analysis of an SO_2 flux times-series from SHV. STFT analysis was then used to investigate further the temporal variability of the cycles in each time-series. By comparing and contrasting the STFT results

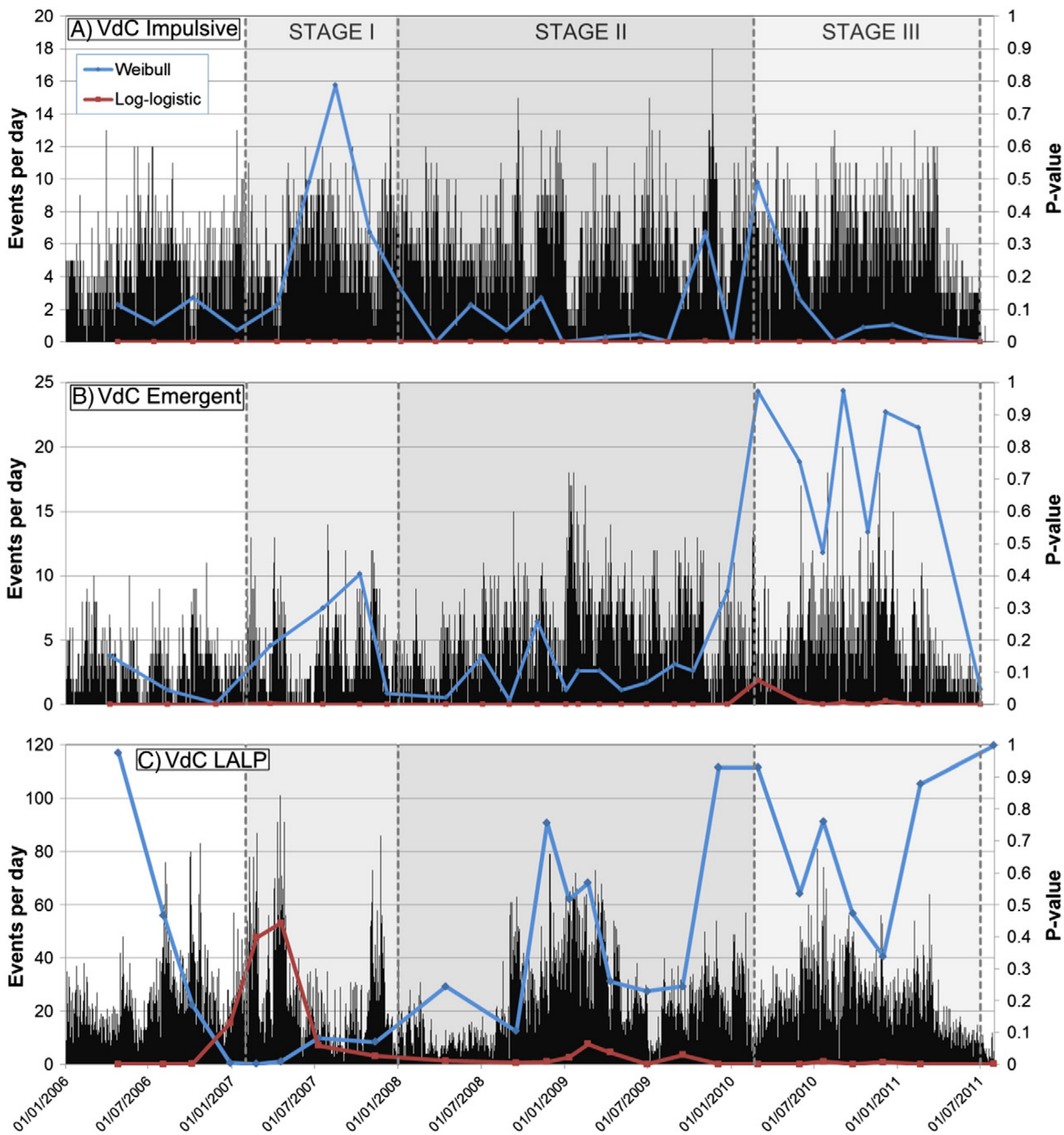

Fig. 7. *P*-values over time for Weibull (solid blue line) and log-logistic (solid red line) fits to event repose intervals and daily event counts (black bars) for (A) impulsive, (B) emergent, and (C) LALP seismicity recorded at Volcán de Colima (VdC). *P*-values are recorded on the date of the youngest repose interval used in their respective bins. Note the different y-axes scales for event counts.

from VdC and SHV it is clear that there are similarities in the long-term behaviour of seismicity at each volcanic system (Figs. 5, 6). One common feature is a range of cycles with ~50-, ~100-, and ~200-day periods. This range may seem harmonic with a fundamental frequency with a period of 50-days, but this cannot be the case as the different cycles rarely, if at all, appear simultaneously. This is seen most clearly in the explosions from VdC (Fig. 5A) where 50-day and 100-day cycles do not appear simultaneously in stage II. Over time, the cycles fluctuate in strength and are only weakly, if at all, correlated to variations in lava dome growth. Cycles with similar periods are seen at both systems, despite the variations in extrusion rate. VdC had much slower rates (<1 $m^3 s^{-1}$; Mueller et al., 2013) than at SHV (2–5.6 $m^3 s^{-1}$ Ryan et al., 2010; Wadge et al., 2010). In Voight et al (1998) the onset of '50-day' cycles in tiltmeter data at SHV were indicated by sudden increases in seismicity or surface activity; this characteristic is not shared by the sub-annual cycles at VdC.

The similarity of the cycles at SHV found here and in previous work using other monitoring parameters (Voight et al., 1998; Nicholson et al., 2013; Odbert et al., 2014) gives confidence in the results. In Odbert et al. (2014), 50-day cycles appear to be much more prevalent in the seismicity than those described in this work and no 100-day cycle is detected in their analysis. The incomplete agreement of results may be due to either a difference in the time-series used (Odbert et al., 2014, analyse total seismic events over the same time-period rather than time-series for each event type), or a methodological difference (Odbert et al., 2014, use Continuous Wavelet Transform) which means that the suitability of each statistical method will need to be more thoroughly assessed in order to understand which is more reliable and the reasons for the differences. Comparing and contrasting the results from both MTM and STFT analysis brought out several key observations (Section 3.1.3). The observation that cycles seen in MTM analysis appear only briefly in the spectrograms produced by STFT, and that the same cycles are often not simultaneous, demonstrates the justification of using the STFT method on the dataset. Without the results from the STFT analysis, the results from the MTM analysis would have been misinterpreted. The remaining observation, that several cycles seen in the MTM analysis have not appeared in the STFT results (and vice versa) cannot be easily explained; it may be that they are methodological artefacts. These observations emphasise the need to explore time-series data using multiple approaches, producing more robust evidence on which to draw conclusions regarding any patterns that may be present.

Before trying to understand the nature of these cycles, we need to consider first the source mechanisms behind each type of seismicity. At VdC, explosions have been shown to be the result of rapidly decompressing magma at a shallow depth (Petrosino et al., 2011; Lavallée et al., 2012). LALP seismicity has been linked to the brittle failure of magma as it passes through the glass transition due to shearing along the conduit walls (Varley et al., 2010a,b). It has also been suggested that LALP events are generated by the movement of volcanic fluids through the volcanic system (Petrosino et al., 2011). At SHV, hybrid and LP seismicity have been suggested to have a similar source mechanism as LALP seismicity at VdC, with brittle failure of magma passing through the glass transition acting as a trigger and resonance producing the low-frequency coda (Neuberg et al., 2006). Volcano-tectonic seismicity is thought to be the expression of brittle failure of rock due to stresses induced by the movement of magma (McNutt, 2005). A common link between all volcano-seismic event types analysed here is the movement of magma and volcanic gas within the volcanic system. Explosions require magma to move to shallow depth before rapidly decompressing and producing gas- and ash-filled clouds at the surface. LALP, long-period and hybrid seismicity require ascending magma for brittle failure or the resonance of volcanic gas within cracks in the system. Volcano-tectonic seismicity is the exception in that it requires stress induced by magma movement with no influence from volcanic gas. This implies that the cycles seen in volcano-seismicity at both VdC and SHV are linked to cyclic motion of magma and volcanic gas/fluid within each volcanic plumbing system; this is discussed further in Section 4.4.

4.2. Long-term cycles in persistence

In common with the results of the STFT analysis, there are clear similarities in the time-evolution of correlation within the seismic time-series at each volcanic system (Figs. 5, 6). With the exception of volcano-tectonic events at SHV, the results show a weak positive relationship between the scaling exponent and seismic event rates; this is clearer at SHV (Fig. 6) where periods of reduced levels of seismicity are correlated with relatively low scaling exponents. The different parameters used for analysis here mean that short-term trends at VdC described by Lachowycz et al. (2013) could not be seen. We use a 50-day moving increment rather than 1-day to avoid the parameter artefact discussed in Section 2.2. However, comparison of our results with that of Lachowycz et al. (2013) suggests that similar long-term trends have been identified.

With the exception of explosion events at VdC (Fig. 5A), the time-series show an approximately annual cycle in one part of their correlation time-series (Figs. 5, 6). These cycles are not clearly seen in the raw data, emphasising that these are annual cycles in the 'roughness' of the time-series, not the activity itself. Observations from Mt St Helens (Mastin, 1994) and SHV (Matthews et al., 2002, 2009), and thermodynamic modelling (Hicks et al., 2010) have shown that rainfall can modulate the processes within active volcanic systems and Lachowycz et al. (2013) cited the same effect to explain similar cycles seen in their analysis of seismicity at VdC and SHV. However, the cycles seen in the time-series here do not correlate with the wet seasons at VdC (June to October; Fig. 8) or SHV (July to December; Fig. 9), and the interpretation requires further investigation. Alvarez-Ramirez et al. (2009) cited quasi-periodic dynamics related to volcano-tectonic events as possibly producing the cycles observed in the scaling exponent of explosions from Popocatépetl volcano (Mexico). While this could apply to SHV, it cannot apply to VdC since volcano-tectonic events have been rare since the beginning of the current eruption (Varley et al., 2010b). The 1.5–2 year cycle described here for VdC explosions (Fig. 5A) contrasts with a shorter annual cycle described by Lachowycz et al. (2013). It may be that combining the Impulsive and Emergent event counts has altered the cycle but it is not clear why this should be the case, considering the similarity in the mechanism of the events (Table A, supplementary file 1). Cycles on a similar timescale have been described at SHV for lava extrusion (Odbert et al., 2014). However, it must be emphasised that the SHV cycles were seen in the time-series data whereas the cycles described here are in terms of long-term correlation within the time-series; thus they are less likely to be produced by a similar process.

There is little correlation between the values of α and the results of the STFT analysis. This suggests that the processes at sub-annual timescales and at annual timescales have no significant effect on each other. However, STFT has been carried out at a finer resolution than DFA due to the parameter artefact effect in the latter and this has likely affected the results somewhat; therefore the comparison of these analyses is somewhat speculative.

4.3. Variations in repose intervals

Variations in strength (i.e. *P*-value) of Weibull and log-logistic models (Fig. 7) suggest changes in processes occurring within the volcanic system. The log-logistic model describes a system with at least two competing processes affecting the measured signals, whereas the Weibull model describes a system where simple failure is dominating the signal (Watt et al., 2007).

The transition from Weibull to log-logistic model behaviour and back (Fig. 7C) can be explained in the context of a transition in the source mechanisms for the seismicity (see Section 4.1 for discussion of

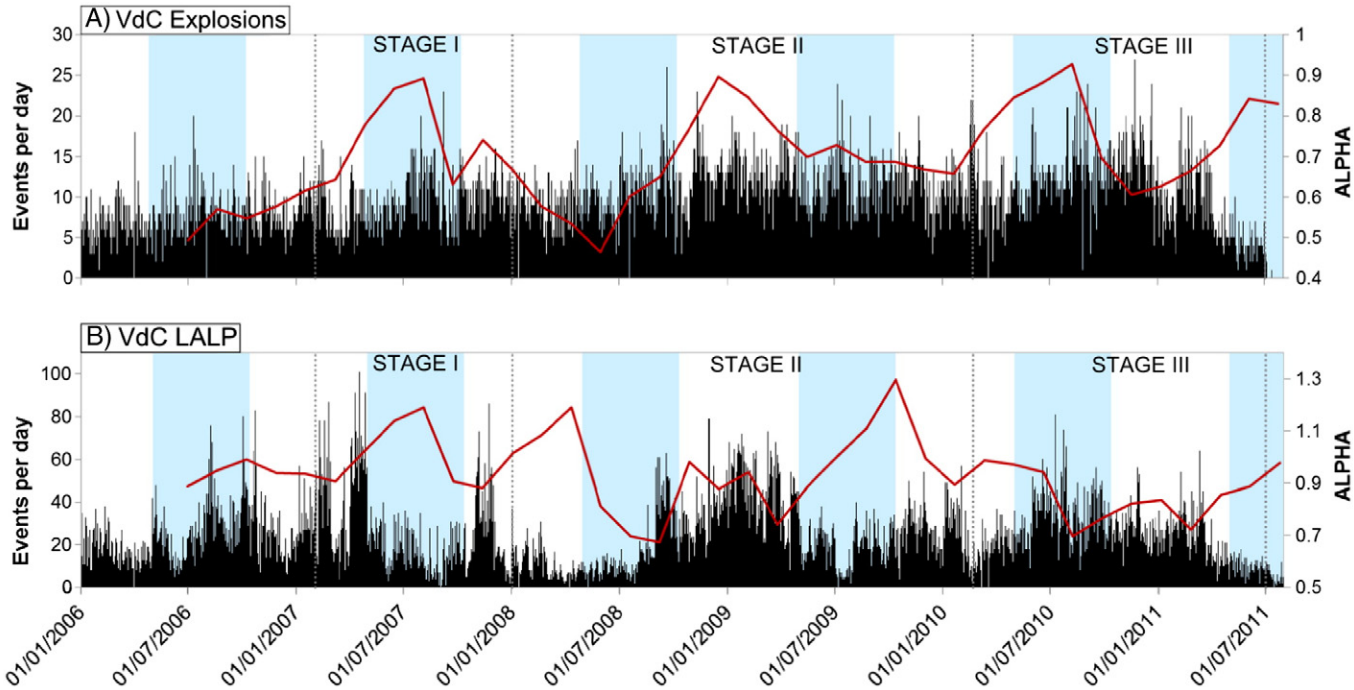

Fig. 8. Daily event counts (black bars) and the DFA scaling exponent values (α; solid red line) from Volcán de Colima (VdC) plotted with the wet seasons during the period of analysis shown (blue areas). The scaling exponent (α) values are plotted at the end of their respective windows of measurement; gaps represent periods where invalid scaling exponents are calculated due to insufficient seismic events.

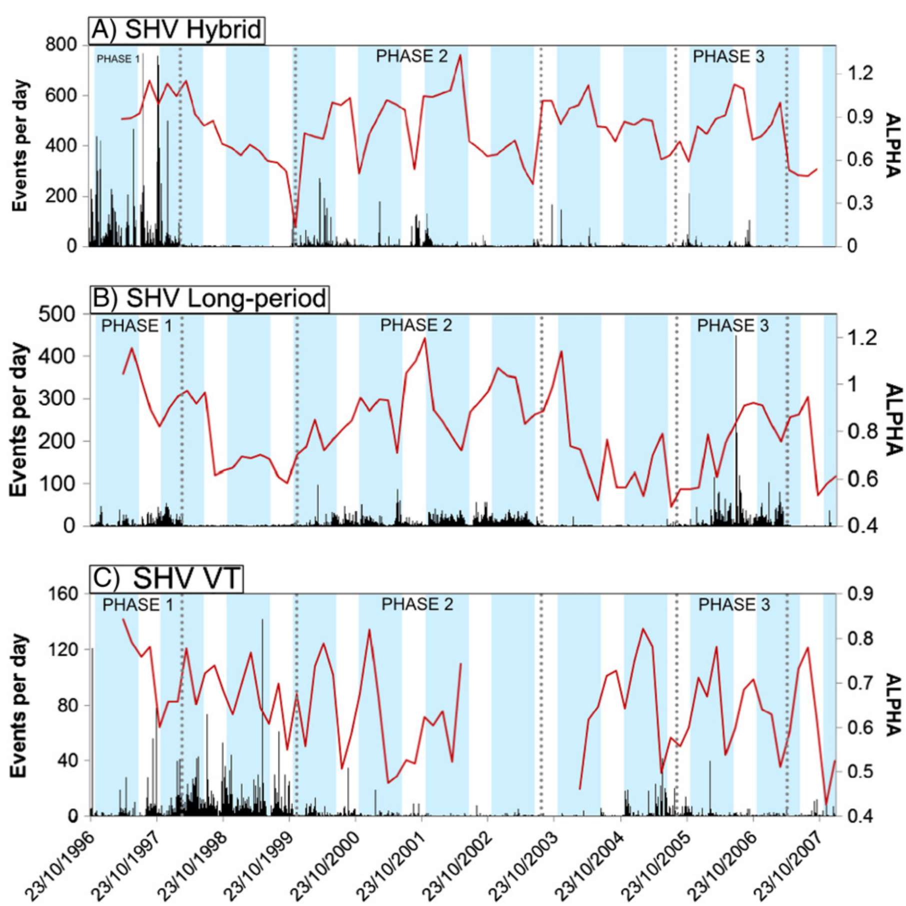

Fig. 9. Daily event counts (black bars) and the DFA scaling exponent values (α; solid red line) from Soufrière Hills volcano (SHV) plotted with the wet seasons during the period of analysis shown (blue areas). The scaling exponent (α) values are plotted at the end of their respective windows of measurement; gaps represent periods where invalid scaling exponents are calculated due to insufficient seismic events.

Table 2
Comparison of known facts at each volcanic system.

	Volcán de Colima[a]	Soufrière Hills volcano[b]
Bulk composition	Andesite	Andesite
Latest activity	1997–2011; Jan. 2013–ongoing.	1995–ongoing
No. of dome building phases	5	5
Example Dome size (m^3)	1.5–2 × 10^6 (2007–2011)	203 × 10^6 (non-dense rock equivalent, 2007)
Storage depth 1 (km)	2.3–6.6	5.5–7.5
Storage depth 2 (km)		12.7–23.5
Storage temperature (°C)	940–1060	820–880
Conduit radius (m)		15 ± 10
Effusion rate ($m^3 s^{-1}$)	>5 (1998–1999, 2004), <1 (2001–2003, 2007–2011)	4.3 (Phase 1), ~2 (Phase 2), 5.6 ± 0.9 (Phase 3)
Pre-eruptive H_2O (wt. %)	≤4.1	4.27 ± 0.5
log fO_2	−10.5 to −12.2	−11.2 to −11.7
Cycle Timescales		
Activity	~100 years in Plinian or sub-Plinian eruptions.	~30 year seismic crisis cycle
Dome growth		2–3 years
Seismicity	50-, 100-, 200-days	3–30 h, 11–16 days, 6–8 weeks, 100-, 200-days.
SO_2		6–8 weeks
Deformation		3–30 h, 6–8 weeks, 2–3 years
Explosions	1–4 h	8–12 h

[a] Luhr and Carmichael (1980), Luhr (2002), Hutchison et al. (2013), Mueller et al. (2013), Reubi et al. (2013) and this study.
[b] Barclay et al. (1998), Devine et al. (1998), Young et al. (1998), Murphy et al. (2000), Lensky et al. (2008), Ridolfi et al. (2010), Ryan et al. (2010), Paulatto et al. (2012), Nicholson et al. (2013) and Odbert et al. (2014).

mechanisms). Most of 2006 is dominated by the Weibull model, implying the LALP record was dominated by a single brittle failure mechanism. Slow magma ascent likely only occurred towards the end of 2006 prior to the onset of dome growth in January 2007. This suggests that the LALP time-series in 2006 is not dominated by brittle failure of magma, but instead the resonance of volcanic fluids by brittle failure of cracks. Immediately prior to the first observation of a dome in February 2007, the log-logistic model becomes more significant suggesting two competing mechanisms. At this time, magma had begun ascending through the volcanic system and LALP seismicity was then produced by both brittle failure of magma and as well as resonance of fluids. The fact that the peak for the log-logistic model occurs after the first few weeks of dome growth suggests that ascending magma was still degassing enough to produce LALP seismicity from resonance of volatiles, ash suspension, or magma melt. The dominance of the Weibull model for most of the 2007–2011 dome growth activity is an indication that the brittle failure mechanism is more prevalent. One way of testing this idea would be to carry out further examination of the families of seismic events, looking for any subtle changes in waveform characteristics during the onset of dome growth. Previously this approach has observed and described the presence of swarms of long-period seismicity associated with explosions occurring at VdC (Varley et al., 2010b; Arámbula-Mendoza et al., 2011). At the end of activity in July 2011, the Weibull model continues to dominate (Fig. 7C) even as activity decreases and ceases.

It is unsurprising that the results for emergent and impulsive events are similar (Fig. 7A, B) since the difference between the generation mechanisms is likely to be minimal (see supplementary file 1). Each event is the expression of sudden and violent release of gas via fractured pathways to the surface (Varley et al., 2010a); the difference being that Emergent events represent a more gradual release of gas, whereas Impulsive events involve a single large fracture dominating the signal. The higher Weibull fit parameter during stages I and III (Fig. 7A, B) suggest that Emergent and Impulsive event repose intervals may be affected by the balance between exogenous and endogenous dome growth, with the exogenous growth and lava lobe effusion promoting Weibull behaviour. This suggests that the change in lava dome growth mechanism slightly affects the generation mechanism for explosions. There are periods when neither probabilistic model fits produce significant *P*-values; e.g. January 2008 to July 2009. The reasons for these periods are unclear, and have no correlation with the results from other methods (Fig. 5A); these periods need to be investigated further.

4.4. Common behaviour at two separate systems

The most important observation to come out of the analysis of seismicity from the two volcanic systems is the broadly common cyclical pattern of behaviour in each system: the ~50-, ~100- and ~200-day cycles in event counts (Section 3.1, Figs. 5, 6). The periods of the cycles described here are broadly consistent with those described in deformation (Voight et al., 1999) and SO_2 flux timeseries (Nicholson et al., 2013) at SHV which suggests that a common process, or a set of common processes, influences the temporal variations of all three datasets. We suggest that the sub-annual cycles (~200 days) may result from cyclic movement of magma within each system (Section 4.1); the challenge now is to model the cause. At SHV, periodic expansion and contraction of an elastic-walled dyke, which acts as a volumetric capacitor to magma storage in the lower conduit has previously been proposed as a mechanism for the 6–8 week (~50-day) cycles (Costa et al., 2007a,b, 2013). The model identifies several key factors that can affect the length of cycles, including magma chamber depth, magma chamber size, dyke width, influx rate from chamber to dyke, and magma rheology. By varying the values of any number of these factors, cycles of ~100 or ~200-days can also be modelled; for example a dyke with width of 60–90 m could produce a 200-day cycle (See Fig. 6B of Costa et al., 2007a). Here, we show that similar cycles are seen in seismicity at VdC, opening speculation that a similar model could potentially be applied to this volcanic system. However, any attempts to model the conduit processes operating at these dome-forming volcanoes must be able to account for the observed cyclic behaviour in seismicity, deformation and SO_2 flux while reconciling the differences and similarities between the two systems (Table 2). The recognition of these parallels in behaviour suggests that it would be worthwhile extending this approach to time-series data from other long-lived dome-forming eruptions. It also suggests the potential of using these techniques as a basis for the development of automated near-real time monitoring tools. These tools would be designed to automatically detect changes in patterns of behaviour that may lead to changes in hazard potential of a volcanic system.

5. Conclusions

We have successfully applied a suite of analytical tools to daily seismic count datasets from Volcán de Colima (VdC) and Soufrière Hills volcano (SHV), providing insights into long-term behaviour within each system. Fast Fourier Transform analysis (Multitaper Method and Short-Term Fourier Transform) revealed temporally variable ~50-, ~100-, and ~200-day cycles that may be linked to variations in magma movement in the volcanic plumbing system. Detrended Fluctuation Analysis showed correlations between the number of seismic events and the long-range power-law correlation (i.e. persistence) of seismicity at each volcanic system; with no clear mechanism to explain it. Probabilistic Distribution Analysis was successfully adapted to track changes in the physical processes affecting the seismicity at VdC. Variations in the strength of Weibull or log-logistic models are attributed to either a transition in source mechanisms or changes in growth mode of the lava dome.

Cyclical patterns of behaviour are well documented at SHV (e.g. Voight et al., 1998; Odbert and Wadge, 2009; Nicholson et al., 2013) and their recognition has stimulated the development of physical models of the volcanic system (e.g. Costa et al., 2007a,b, 2012; Thomas and Neuberg, 2012). These physical models in turn, have the potential to inform future assessments of hazards as the nature of the eruption changes through time. Our analysis has revealed some broad-scale similarities in behaviour between SHV and VdC. These results imply that there is potential for the development of a general physical model of the sub-surface processes that are responsible for the cyclical patterns of behaviour at dome-forming volcanoes. The recognition of some common behavioural patterns between time-series of geophysical monitoring data also demonstrates the potential for the development of tools for automated near-real time monitoring, and for their application to hazard detection at multiple volcanic systems.

Acknowledgements

The data analysed in this study were provided by Red Sísmica de Colima and the Centro de Intercambio e investigación en Vulcanolgía of the Universidad de Colima (with specific thanks to Gabriel A. Reyes-Dávila), and the Montserrat Volcano Observatory. We also thank S. Lachowycz (University of Oxford) for assistance with DFA, Dr S. Watt (University of Southampton) for advice on PDA, and Dr M. Rodgers (University of Oxford) for help reviewing the manuscript. NRV has been supported by grants from the Universidad de Colima FRABA 668/10, 768/11, 66/13. DMP and TAM are supported by and contribute to the NERC National Centre for Earth Observation 'Dynamic Earth and Geohazards' group and also the NERC/ESRC 'Strengthening Resilience in Volcanic Areas' project (NE/J020001/1 and NE/J020051/1). TAM further acknowledges the Leverhulme Trust for financial support towards this project. We thank Geoff Wadge and Sandro Aiuppa for their observations that helped make this a much improved paper.

Appendix A. Supplementary data

Supplementary data to this article can be found online at http://dx.doi.org/10.1016/j.jvolgeores.2014.07.013.

References

Alvarez-Ramirez, J., Sosa, E., Rodriguez, E., 2009. Assessing temporal-dependent correlations in the 2000–2008 Popocatepetl exhalation sequence by using detrended fluctuation analysis. J. Volcanol. Geotherm. Res. 186, 426–431.

Arámbula-Mendoza, R., Lesage, P., Valdés-González, C., Varley, N.R., Reyes-Dávila, G., Navarro, C., 2011. Seismic activity that accompanied the effusive and explosive eruptions during the 2004–2005 period at Volcán de Colima, Mexico. J. Volcanol. Geotherm. Res. 205, 30–46.

Barclay, J., Rutherford, M.J., Carroll, M.R., Murphy, M.D., Devine, J.D., Gardner, J., Sparks, R.S.J., 1998. Experimental phase equilibria constraints on pre-eruptive storage conditions of the Soufriere Hills magma. Geophys. Res. Lett. 25, 3437–3440.

Butterworth, S., 1930. Theory of filter amplifiers. Exp. Wirel. Wirel. Eng. 7, 536–541.

Chouet, B.A., 1996. Long-period volcano seismicity: its source and use in eruption forecasting. Nature 380, 309–316.

Chouet, B.A., Matoza, R.S., 2013. A multi-decadal view of seismic methods for detecting precursors of magma movement and eruption. J. Volcanol. Geotherm. Res. 252, 108–175.

Chouet, B.A., Page, R.A., Stephens, C.D., Lahr, J.C., Power, J.A., 1994. Precursory swarms of long-period events at Redoubt Volcano (1989–1990), Alaska: their origin and use as a forecasting tool. J. Volcanol. Geotherm. Res. 62, 95–135.

Connor, C.B., Sparks, R.S.J., Mason, R.M., Banadonna, C., Young, S.R., 2003. Exploring links between physical and probabilistic models of volcanic eruptions: the Soufriere Hills Volcano, Montserrat. Geophys. Res. Lett. 30, 1701–1704.

Costa, A., Melnik, O., Sparks, R.S.J., 2007a. Controls of conduit geometry and wallrock elasticity on lava dome eruptions. Earth Planet. Sci. Lett. 260, 137–151.

Costa, A., Melnik, O., Sparks, R.S.J., Voight, B., 2007b. Control of magma flow in dykes on cyclic lava dome extrusion. Geophys. Res. Lett. 34, L02303.

Costa, A., Wadge, G., Melnik, O., 2012. Cyclic extrusion of a lava dome based on a stick-slip mechanism. Earth Planet. Sci. Lett. 337–338, 39–46.

Costa, A., Wadge, G., Stewart, R., Odbert, H., 2013. Coupled subdaily and multiweek cycles during the lava dome eruption of Soufrière Hills Volcano, Montserrat. J. Geophys. Res. Solid Earth 118, 1895–1903.

Currenti, G., Del Negro, C., Lapenna, V., Telesca, L., 2005. Fluctuation analysis of the hourly time variability of volcano-magnetic signals recorded at Mt. Etna Volcano, Sicily (Italy). Chaos, Solitons Fractals 23, 1921–1929.

Danielson, G.C, Lanczos, C., 1942. Some improvements in practical Fourier analysis and their application to X-ray scattering from liquids. J. Franklin Inst. 233, 365.

De Bélizal, É., Lavigne, F., Gaillard, J.C., Grancher, D., Pratomo, I., Komorowski, J.-C., 2012. The 2007 eruption of Kelut volcano (East Java, Indonesia): phenomenology, crisis management and social response. Geomorphology 136, 165–175.

Denlinger, R.P., Hoblitt, R.P., 1999. Cyclic eruptive behavior of silicic volcanoes. Geology 27, 459–462.

Devine, J.D., Rutherford, M.J., Gardner, J.E., 1998. Petrologic determination of ascent rates for the 1995–1997 Soufriere Hills Volcano andesitic magma. Geophys. Res. Lett. 25, 3673–3676.

Druitt, T.H., Young, S.R., Baptie, B., Bonadonna, C., Calder, E.S., Clarke, A.B., Cole, P.D., Harford, C.L., Herd, R.A., Luckett, R., Ryan, G., Voight, B., 2002. Episodes of cyclic Vulcanian explosive activity with fountain collapse at Soufriere Hills Volcano, Montserrat. Geol. Soc. Lond. Mem. 21, 281–306.

Ghil, M., Allen, M.R., Dettinger, M.D., Ide, K., Kondrashov, D., Mann, M.E., Robertson, A.W., Saunders, A., Tian, Y., Varadi, F., Yiou, P., 2002. Advanced spectral methods for climatic time series. Rev. Geophys. 40, 1003.

Harrington, R.M., Brodsky, E.E., 2007. Volcanic hybrid earthquakes that are brittle-failure events. Geophys. Res. Lett. 34.

Harris, A.J.L., Rose, W.I., Flynn, L.P., 2003. Temporal trends in lava dome extrusion at Santiaguito 1922–2000. Bull. Volcanol. 65, 77–89.

Herd, R.A., Edmonds, M., Bass, V.A., 2005. Catastrophic lava dome failure at Soufrière Hills Volcano, Montserrat, 12–13 July 2003. J. Volcanol. Geotherm. Res. 148, 234–252.

Hicks, P.D., Matthews, A.J., Cooker, M.J., 2010. Triggering of a volcanic dome collapse by rainwater infiltration. J. Geophys. Res. 115, B09212.

Hutchison, W., Varley, N.R., Pyle, D.M., Mather, T.A., Stevenson, J.A., 2013. Airborne thermal remote sensing of the Volcan de Colima (Mexico) lava dome from 2007 to 2010. Geol. Soc. Lond. Spec. Publ. 380, 203–228.

Jaquet, O., Carniel, R., 2003. Multivariate stochastic modelling: towards forecasts of paroxysmal phases at Stromboli. J. Volcanol. Geotherm. Res. 128, 261–271.

Jaquet, O., Carniel, R., Sparks, S., Thompson, G., Namar, R., Di Cecca, M., 2006. DEVIN: a forecasting approach using stochastic methods applied to the Soufrière Hills Volcano. J. Volcanol. Geotherm. Res. 153, 97–111.

Kilburn, C., 2012. Precursory deformation and fracture before brittle rock failure and potential application to volcanic unrest. J. Geophys. Res. 117, 1–12.

Lachowycz, S.M., Pyle, D.M., Mather, T.A., Varley, N.R., Odbert, H.M., Cole, P.D., Reyes-Dávila, G.A., 2013. Long-range correlations identified in time-series of volcano seismicity during dome-forming eruptions using detrended fluctuation analysis. J. Volcanol. Geotherm. Res. 264, 197–209.

Lahr, J.C., Chouet, B.A., Stephens, C.D., Power, J.A., Page, R.A., 1994. Earthquake classification, location, and error analysis in a volcanic environment: implications for the magmatic system of the 1989–1990 eruptions at Redoubt Volcano, Alaska. J. Volcanol. Geotherm. Res. 62, 137–151.

Lavallée, Y., Varley, N.R., Alatorre-Ibargüengoitia, M.A., Hess, K.-U., Kueppers, U., Mueller, S., Ruchard, D., Scheu, B., Spieler, O., Dingwell, D.B., 2012. Magmatic architecture of dome-building eruptions at Volcán de Colima, Mexico. Bull. Volcanol. 74, 249–260.

Lensky, N.G., Sparks, R.S.J., Navon, O., Lyakhovsky, V., 2008. Cyclic activity at Soufriere Hills Volcano, Montserrat: degassing-induced pressurization and stick-slip extrusion. Geol. Soc. Lond. Spec. Publ. 307, 169–188.

Linde, A.T., Sacks, S., Hidayat, D., Voight, B., Clarke, A., Elsworth, D., Mattioli, G., Malin, P., Shalev, E., Sparks, S., Widiwijayanti, C., 2010. Vulcanian explosion at Soufrière Hills Volcano, Montserrat on March 2004 as revealed by strain data. Geophys. Res. Lett. 37 (n/a–n/a).

Loughlin, S.C., Luckett, R., Ryan, G., Christopher, T., Hards, V., De Angelis, S., Jones, L., Strutt, M., 2010. An overview of lava dome evolution, dome collapse and cyclicity at Soufrière Hills Volcano, Montserrat, 2005–2007. Geophys. Res. Lett. 37, L00E16.

Luckett, R., Baptie, B., Ottemoller, L., Thompson, G., 2007. Seismic monitoring of the Soufrière Hills Volcano, Montserrat. Seismol. Res. Lett. 78, 192–200.

Luckett, R., Loughlin, S., De Angelis, S., Ryan, G., 2008. Volcanic seismicity at Montserrat, a comparison between the 2005 dome growth episode and earlier dome growth. J. Volcanol. Geotherm. Res. 177, 894–902.

Luhr, J.F., 2002. Petrology and geochemistry of the 1991 and 1998–1999 lava flows from Volcan de Colima, Mexico: implications for the end of the current eruptive cycle. J. Volcanol. Geotherm. Res. 117, 169–194.

Luhr, J.F., Carmichael, I.S.E., 1980. The Colima Volcanic Complex, Mexico: Part I. Post-Caldera Andesites From Volcan Colima. Contrib. Mineral. Petrol. 71, 343–372.

Mann, M.E., Lees, J.M., 1996. Robust estimation of background noise and signal detection in climatic time series. Clim. Chang. 33, 409–445.

Massey, F.J., 1951. The Kolmogorov–Smirnov Test for Goodness of fit. J. Am. Stat. Assoc. 46, 68–78.
Mastin, L.G., 1994. Explosive tephra emissions at Mount St . Helens, 1989–1991: the violent escape of magmatic gas following storms? Geol. Soc. Am. Bull. 106, 175–185.
Matthews, A.J., Barclay, J., Carn, S., Thompson, G., Alexander, J., Herd, R., Williams, C., 2002. Rainfall-induced volcanic activity on Montserrat. Geophys. Res. Lett. 29, 3–6.
Matthews, A.J., Barclay, J., Johnstone, J.E., 2009. The fast response of volcano-seismic activity to intense precipitation: triggering of primary volcanic activity by rainfall at Soufrière Hills Volcano, Montserrat. J. Volcanol. Geotherm. Res. 184, 405–415.
McNutt, S.R., 2005. Volcanic seismology. Annu. Rev. Earth Planet. Sci. 33, 461–491.
Melnik, O., Sparks, R.S.J., 2005. Controls on conduit magma flow dynamics during lava dome building eruptions. J. Geophys. Res. 110, B02209.
Mueller, S.B., Varley, N.R., Kueppers, U., Lesage, P., Reyes Davila, G.Á., Dingwell, D.B., 2013. Quantification of magma ascent rate through rockfall monitoring at the growing/collapsing lava dome of Volcán de Colima, Mexico. Solid Earth 4, 201–213.
Murphy, M.D., Sparks, R.S.J., Barclay, J., Carroll, M.R., Brewer, T.S., 2000. Remobilization of andesite magma by intrusion of mafic magma at the Soufriere Hills Volcano, Montserrat, West Indies. J. Petrol. 41, 21–42.
Nakada, S., Shimizu, H., Ohta, K., 1999. Overview of the 1990–1995 eruption at Unzen Volcano. J. Volcanol. Geotherm. Res. 89, 1–22.
Neuberg, J., 2000. Characteristics and causes of shallow seismicity in andesite volcanoes. Philos. Trans. R. Soc. A 358, 1533–1546.
Neuberg, J.W., Tuffen, H., Collier, L., Green, D., Powell, T., Dingwell, D., 2006. The trigger mechanism of low-frequency earthquakes on Montserrat. J. Volcanol. Geotherm. Res. 153, 37–50.
Nicholson, E.J., Mather, T.A., Pyle, D.M., Odbert, H.M., Christopher, T., 2013. Cyclical patterns in volcanic degassing revealed by SO2 flux timeseries analysis: an application to Soufrière Hills Volcano, Montserrat. Earth Planet. Sci. Lett. 375, 209–221.
Norton, G.E., Watts, R.B., Voight, B., Mattioli, G.S., Herd, R.A., Young, S.R., Devine, G.E., Aspinall, W.P., Bonadonna, C., Baptie, B.J., Edmonds, M., Jolly, A.D., Loughlin, S.C., Luckett, R., Sparks, S.J., 2002. Pyroclastic flow and explosive activity at Soufriere Hills Volcano, Montserrat, during a period of virtually no magma extrusion (March 1998 to November 1999). Geol. Soc. Lond. Mem. 21, 467–481.
Odbert, H.M., Wadge, G., 2009. Time series analysis of lava flux. J. Volcanol. Geotherm. Res. 188, 305–314.
Odbert, H.M., Stewart, R.C., Wadge, G., 2014. Cyclic phenomena at the Soufriere Hills Volcano, Montserrat. Geol. Soc. Lond. Mem. 39, 41–60.
Paulatto, M., Annen, C., Henstock, T.J., Kiddle, E., Minshull, T.A., Sparks, R.S.J., Voight, B., 2012. Magma chamber properties from integrated seismic tomography and thermal modeling at Montserrat. Geochem. Geophys. Geosyst. 13.
Peng, C.-K., Buldyrev, V., Havlin, S., Simons, M., Stanley, H.E., Goldberger, A.L., 1994. Mosaic organisation of DNA nucleotides. Phys. Rev. E. 49, 1685–1689.
Percival, D., Walden, A., 1993. Spectral Analysis for Physical Applications: Multitaper and Conventional Univeriate Techniques. Cambridge University Press.
Petrosino, S., Cusano, P., Rocca, M., Galluzzo, D., Orozco-Rojas, J., Bretón, M., Ibáñez, J., Pezzo, E., 2011. Source location of long period seismicity at Volcàn de Colima, México. Bull. Volcanol. 73, 887–898.
Pyle, D.M., 1998. Forecasting sizes and repose times of future extreme volcanic events. Geology 26, 367–370.
Pyle, D.M., Mather, T.A., Biggs, J., 2013. Remote sensing of volcanoes and volcanic processes: integrating observation and modelling — introduction. Geol. Soc. Lond. Spec. Publ. 380, 1–13.
Reubi, O., Blundy, J., Varley, N.R., 2013. Volatiles contents, degassing and crystallisation of intermediate magmas at Volcan de Colima, Mexico, inferred from melt inclusions. Contrib. Mineral. Petrol. 165, 1087–1106.
Ridolfi, F., Renzulli, A., Puerini, M., 2010. Stability and chemical equilibrium of amphibole in calc-alkaline magmas: an overview, new thermobarometric formulations and application to subduction-related volcanoes. Contrib. Mineral. Petrol. 160, 45–66.
Ryan, G.A., Loughlin, S.C., James, M.R., Jones, L.D., Calder, E.S., Christopher, T., Strutt, M.H., Wadge, G., 2010. Growth of the lava dome and extrusion rates at Soufrière Hills Volcano, Montserrat, West Indies: 2005–2008. Geophys. Res. Lett. 37, L00E08.
Siswowidjoyo, S., Suryo, I., Yokoyama, I., 1995. Magma eruption rates of Merapi volcano, Central Java, Indonesia during one century (1890–1992). Bull. Volcanol. 57, 111–116.
Sparks, R.S.J., 2003. Forecasting volcanic eruptions. Earth Planet. Sci. Lett. 210, 1–15.
Surono, Jousset, P., Pallister, J., Boichu, M., Buongiorno, M.F., Budisantoso, A., Costa, F., Andreastuti, S., Prata, F., Schneider, D., Clarisse, L., Humaida, H., Sumarti, S., Bignami, C., Griswold, J., Carn, S., Oppenheimer, C., Lavigne, F., 2012. The 2010 explosive eruption of Java's Merapi volcano — a "100-year" event. J. Volcanol. Geotherm. Res. 241-242, 121–135.
Swanson, D., Holcomb, R., 1990. Regularities in growth of the Mount St Helens dacite dome, 1980–1986. In: Fink, J. (Ed.), Lava Flows and Dome: Emplacement Mechanisms and Hazard Implications. Iavcei Proceedings in Volcanology. vol. 2, pp. 3–24.
Thomas, M.E., Neuberg, J., 2012. What makes a volcano tick—a first explanation of deep multiple seismic sources in ascending magma. Geology 40, 351–354.
Thomson, D.J., 1982. Spectrum estimation and harmonic analysis. Proc. IEEE 70, 1055–1096.
Varley, N.R., Johnson, J., Ruiz, M., Reyes, G., Martin, K., 2006. Applying statistical analysis to understanding the dynamics of volcanic explosions. In: Mader, H.M., Coles, S.G., Connor, C.B., Connor, L.J. (Eds.), Statistics in Volcanology. Geological Society, London, pp. 57–76.
Varley, N.R., Arámbula-Mendoza, R., Reyes-Dávila, G., Sanderson, R., Stevenson, J., 2010a. Generation of Vulcanian activity and long-period seismicity at Volcán de Colima, Mexico. J. Volcanol. Geotherm. Res. 198, 45–56.
Varley, N.R., Arámbula-Mendoza, R., Reyes-Dávila, G., Stevenson, J., Harwood, R., 2010b. Long-period seismicity during magma movement at Volcán de Colima. Bull. Volcanol. 72, 1093–1107.
Voight, B., Hoblitt, R.P., Clarke, A.B., Lockhart, A.B., Miller, A.D., Lynch, L., Mcmahon, J., 1998. Remarkable cyclic ground deformation monitored in real-time on Montserrat, and its use in eruption forecasting. Geophys. Res. Lett. 25, 3405–3408.
Voight, B., Sparks, R.S.J., Miller, A.D., Stewart, R.C., Hoblitt, R.P., Clarke, A., Ewart, J., Aspinall, W.P., Baptie, B., Calder, E.S., Cole, P.D., Druitt, T.H., Hartford, C., Herd, R.A., Jackson, P., Lejeune, A.M., Lockhart, A.B., Loughlin, S.C., Luckett, R., Lynch, L., Norton, G.E., Robertson, R., Watson, I.M., Watts, R., Young, S.R., 1999. Magma flow instability and cyclic activity at Soufriere Hills Volcano, Montserrat, British West Indies. Science 283 (80), 1138–1142.
Wadge, G., Herd, R., Ryan, G., Calder, E.S., Komorowski, J.-C., 2010. Lava production at Soufrière Hills Volcano, Montserrat: 1995–2009. Geophys. Res. Lett. 37, 1–5.
Watt, S.F.L., Mather, T.A., Pyle, D.M., 2007. Vulcanian explosion cycles: patterns and predictability. Geology 35, 839.
Young, S.R., Sparks, R.S.J., Aspinall, W.P., Lynch, L.L., Miller, A.D., Robertson, R.E.A., Shepherd, J.B., 1998. Overview of the eruption of Soufriere Hills Volcano, Montserrat, 18 July 1995 to December 1997. Geophys. Res. Lett. 25, 3389–3392.